Utilizing Pansharpened LANDSAT 7 Imagery to Detect Urban Change in the Vancouver Census Metropolitan Area: 1999-2002

by

Kevin M. Finney

A Research Paper

presented to Ryerson University

in partial fulfillment of the requirements for the degree of

Master of Spatial Analysis

A joint program with the University of Toronto

Toronto, Ontario, Canada

Author's Declaration

I hereby declare that I am the sole author of this Research Paper.

I authorize Ryerson University to lend this Research Paper to other institutions or individuals for purposes of scholarly research.

_____

Kevin M. Finney

Abstract

The Vancouver Census Metropolitan Area (CMA) has experienced steady growth in recent years. These growth patterns, common to many metropolitan areas, are visible throughout the region using medium to high-resolution satellite imagery. Enhanced Thematic Mapper Plus (ETM+) data from Landsat 7 were put through the PANSHARP image fusion process. An urban change detection analysis for the Vancouver CMA was then performed for a three year period from 1999-2002. Unsupervised classification methods and image differencing techniques allowed for the determination of urban development areas. Change parameters revealed that the CMA region has experienced a yearly average of 5.87km^2 of development, with the majority occurring in areas that correspond to the region's growth strategy. With an overall classification accuracy of approximately 90%, pansharpened imagery allowed for the clear distinction of land cover classes and proved to be an effective tool for detecting urban development.

Acknowledgements

First and foremost, I would like to express considerable appreciation to my advisor, Dr. Wayne Forsythe, for his dedication and help over the entire course of this paper. His timely advice and continuous support made the completion of this paper possible and provided me with the motivation needed to complete this paper on time.

I would also like to thank my Mom and Dad for both their moral and financial support throughout my graduate studies. Without them, this paper would not have been possible and their assistance will never be forgotten.

Table of Contents

List of Tables

List of Figures

List of Acronyms

CCS	Consolidated Census Subdivision
CMA	Census Metropolitan Area
DEM	Digital Elevation Model
ETM+	Enhanced Thematic Mapper Plus
GIS	Geographic Information System
GVRD	Greater Vancouver Regional District
LRSP	Liveable Region Strategic Plan
MSS	Landsat Multi-Spectral Scanner
NDVI	Normalized Difference Vegetation Index
PC1	Principal Component One
PCA	Principal Component Analysis
SPOT	Satellite Probatoire d'Observation de la Terre
TM	Thematic Mapper

Chapter 1: Introduction

Change detection can be broadly defined as the process of identifying differences in the state of an object or phenomenon by observing it at different times (Singh, 1989). Essentially, change detection involves the ability to quantify temporal effects using multi-temporal data sets. Because of the advantages of repetitive data acquisition, its synoptic view, and digital formats suitable for computer processing, remotely sensed data have become the major data source for different change detection applications over the past decades (Lu *et al.*, 2003). Traditionally, the majority of change detection applications were focused on natural environments, but in recent years advancements in image acquisition and quality have allowed urban environments to be studied in more detail. While conventional aerial photographs possess the ability to detect change over relatively small areas at a reasonable cost, satellite imagery has proven to be a more cost effective method for larger region applications (Atkinson and Tate, 2000). Advances in automated change detection techniques, coupled with improvements to image fusion/sharpening methods, have widened the spectrum for urban change detection analysis. Effective image fusion techniques extend the application potential of remotely sensed images as they retain both high-spatial and high-spectral resolutions, characteristics that are vital for accurate change detection studies of urban environments (Zhang, 2004).

1.1 *History of Vancouver, British Columbia*

In 1886, the City of Vancouver was officially incorporated with a population of 1000 people (Discover Vancouver, 2004). Since that time, the city has experienced tremendous growth and the once densely forested area has been transformed into a thriving urban core that contains approximately 546,000 people as reported in the 2001

Census, serving as the foundation for the Vancouver Census Metropolitan Area (CMA) (Statistics Canada, 2001) - (Figure 1.1).

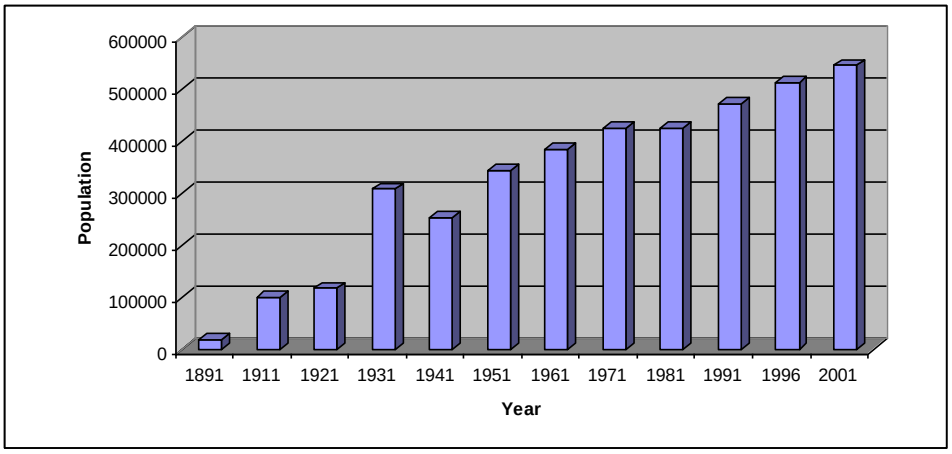

Figure 1.1: City of Vancouver Population History: 1891-2001

With the exception of a few brief periods, Vancouver has always experienced healthy population growth since its inception. The major factor driving population growth in this area has been migration (British Columbia Statistics, 1997).

Generally speaking, the recession of 1982 resulted in the migration of a large share of population away from BC's smaller resource-based communities in favour of regions where employment prospects were more favourable such as the large Metropolitan centres of Vancouver and Victoria. This, coupled with the increasing importance of the service sector, resulted in declining populations in outlying areas in favour of the province's larger metropolitan regions (British Columbia Statistics, 1997). As has been the case in the past, the Vancouver region, with a well-diversified economic base will likely experience more consistent and higher population growth in the future. However, while the population of the Vancouver area is expected to grow larger, it will also grow older as the baby boomers set into the retirement years and a natural decrease is imminent from the existing population base.

1.2 *Study Area*

The Vancouver Census Metropolitan Area (CMA) - (Figure 1.2), closely resembling the Greater Vancouver Regional District (GVRD) - (Figure 1.3) is located in the southwest corner of mainland British Columbia. The CMA is comprised of nine Consolidated Census Subdivisions (CCS).

Between 1991 and 1996, Vancouver was the fastest growing metropolitan area in Canada, but shifted to fifth place in the second half of the 1990's. Immigration data released by Statistics Canada revealed that 189,660 immigrants to Canada settled in Greater Vancouver between 1991 and 1996 (Statistics Canada, 1996). At the same time, the region's total population grew by 229,075 people, from 1,602,590 in 1991 to 1,831,665 in 1996. This means that international immigration accounted for 82.8% of the region's growth between 1991 and 1996. While the inflow of international migrants into the region was down 20,000 from the record highs posted in the previous 1991-1996 period, regional gains in immigrant residents between 1996 and 2001 were the second highest ever recorded over a five year period. The decline in international immigration during the latter part of the 1990's was primarily due to the curtailment of immigration flows from Hong Kong (GRVD Policy and Planning, 2003). During the 1991-1996 census period leading up to Hong Kong's 1997 repatriation with the People's Republic of China, Greater Vancouver received 44,700 Hong Kong immigrants, but levels fell drastically to 15,700 in the five year period following the transfer of sovereignty (GRVD Policy and Planning, 2003).

Figure 1.2: Location of the Vancouver CMA Study Area. (A) Geographical location of the Vancouver CMA in provincial context (*Source*: Graphic Maps, 2004); (B) Nine CCS that comprise the Vancouver CMA (*Source*: DMTI Spatial, 2004).

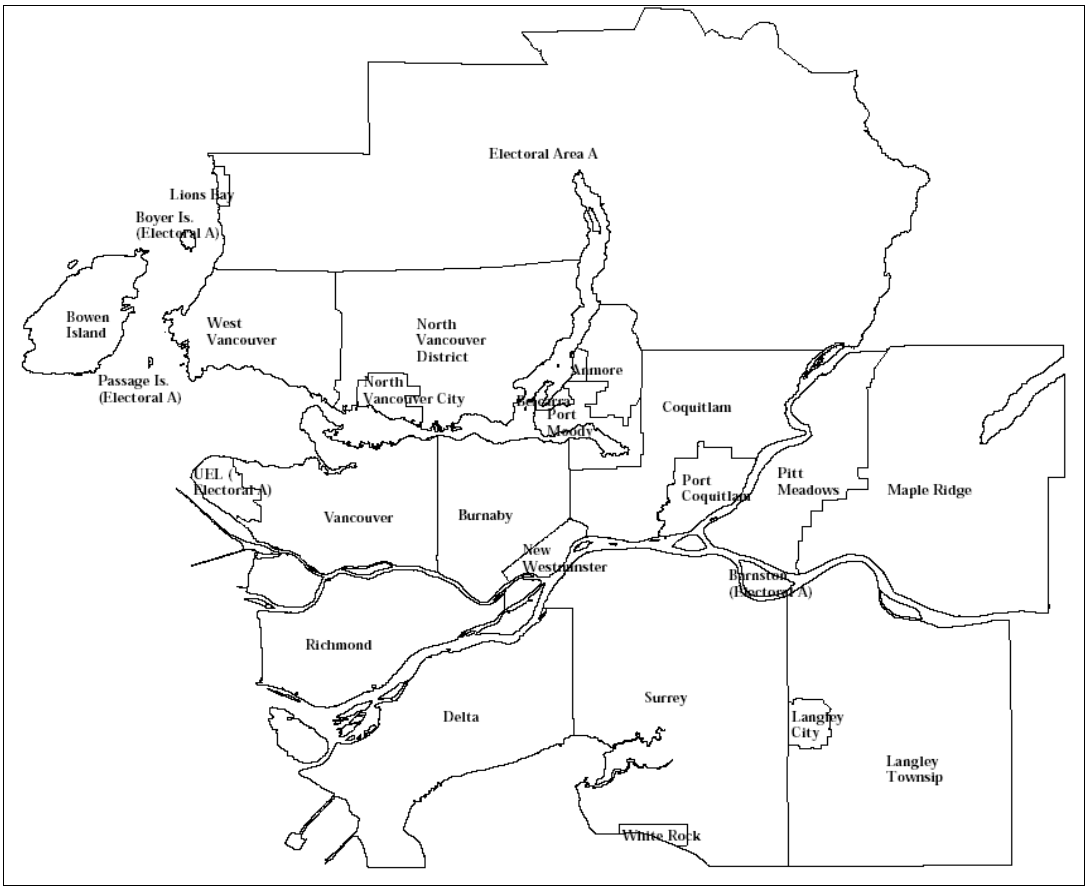

Figure 1.3: Overview of the Greater Vancouver Regional District (GVRD) – (*Source*: GRVD, 2004).

Overall, between 1996 and 2001, BC's population grew by 4.9% (183,238 people), slightly higher than the national rate of 4.0%. Within BC, the focus of growth shifted, towards the three CMAs of Vancouver, Victoria, and Abbotsford. While these three areas accounted for 95% of the increase in population overall, 85% of this growth was in the Vancouver CMA alone. Even with the lower growth rate, the Vancouver CMA added over 155,000 people in five years, the equivalent of adding a municipality the size of Richmond BC (City of Vancouver, 2001). This population boom led to a significant increase in housing growth rates, depicted in Figure 1.4 below.

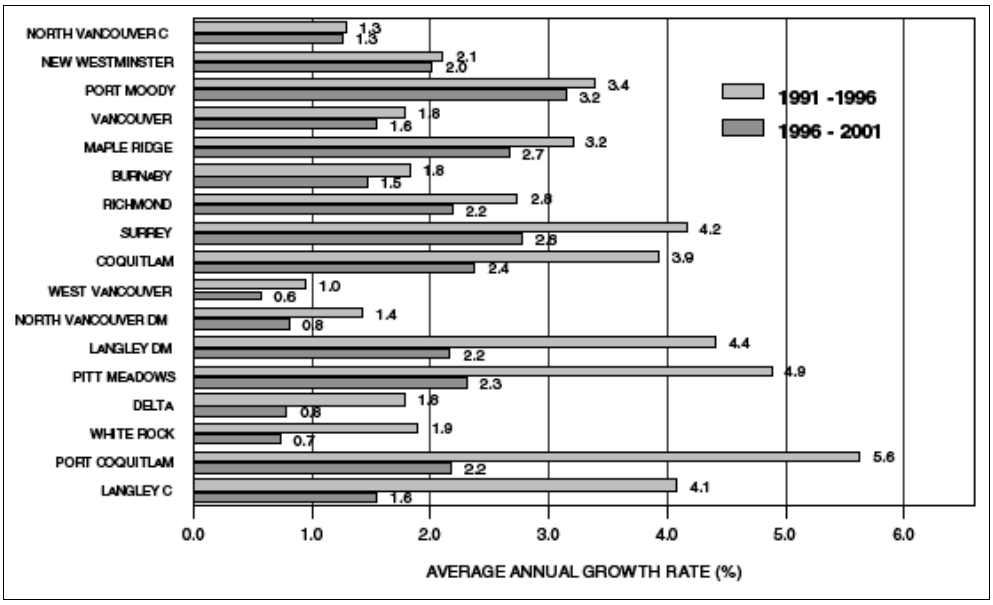

Figure 1.4: Average Annual Housing Growth Rates, 1991-1996 & 1996 – 2001
Source: City of Vancouver, 2001.

1.3 *Vancouver's Liveable Region Strategic Plan (LRSP)*

Adopted in 1996, the Liveable Region Strategic Plan (LRSP) is Greater Vancouver's regional growth strategy to ensure the region's future sustainability. The primary goal is to help maintain regional liveability and protect the environment in the face of anticipated growth in Greater Vancouver (GVRD, 1996). The LRSP calls for concentration of a larger share of population, and correspondingly of new housing, in the Burrard Peninsula, the North East Sector, North Surrey and North Delta, in order to allow more people to live closer to their workplaces. Furthermore, the Plan encourages more ground-oriented housing within this area of compact growth. Housing trends confirm the region's increasing appetite for ground-oriented, medium density housing forms, but the challenge remains to accommodate more of the total additional housing required regionally within the growth concentration area defined by the Plan, delineated by the white areas in Figure 1.5 below (GVRD Planning Department, 1998).

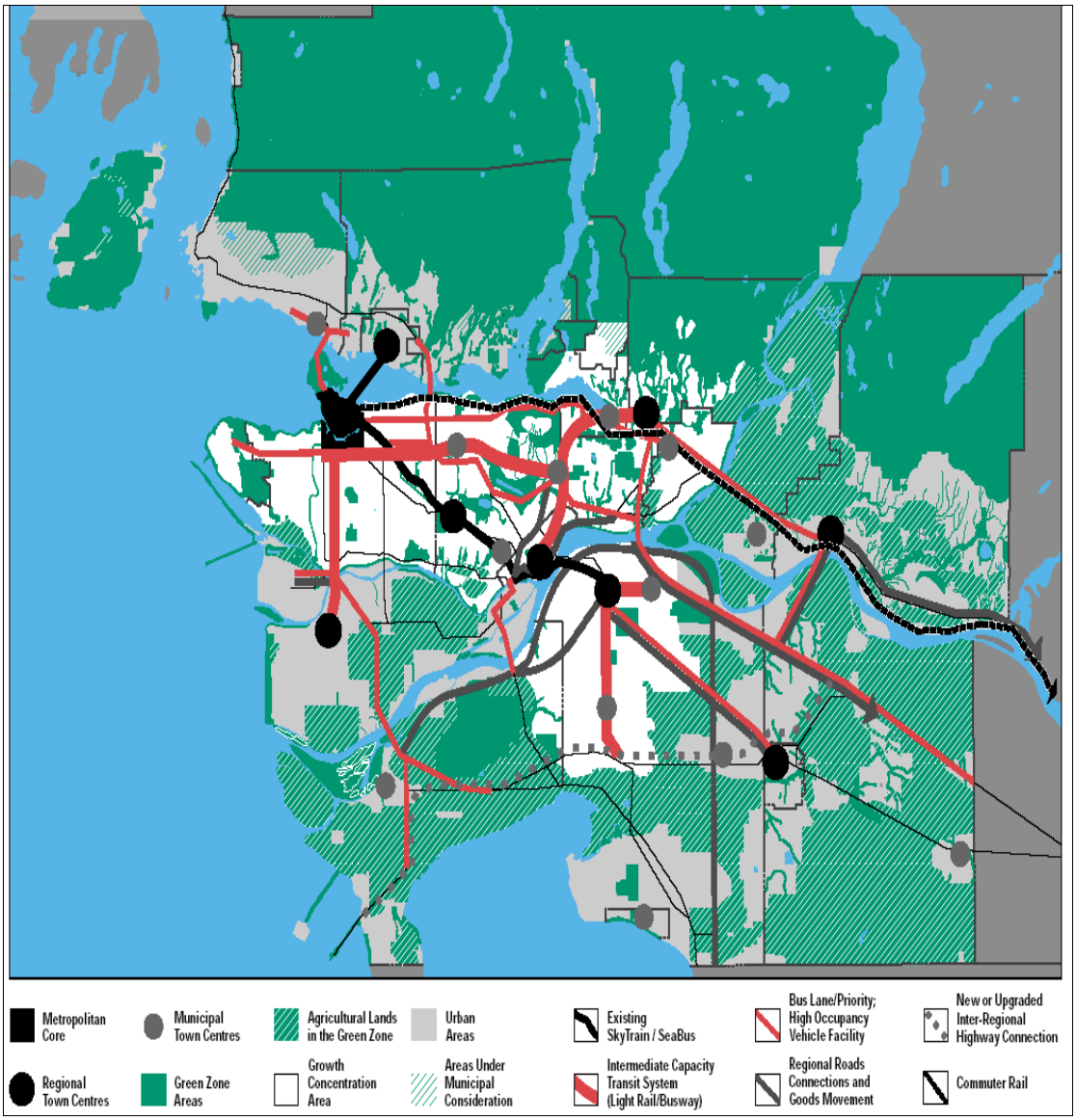

Figure 1.5: LRSP Concept Map (*Source*: GVRD, 2004).

1.4 *Problem Statement*

The Vancouver CMA has experienced enormous growth over the past decade. Between 1991 and 1996, Vancouver was the fastest growing metropolitan area in Canada, but shifted to fifth place in the second half of the 1990's. Despite the lower growth rate, the population of the Vancouver CMA still increased by over 155,000 people in five years, placing additional pressures on the area's infrastructure and existing housing resources (Northwest Environmental Watch, 2002).

As urbanization continues to extend from central Vancouver, the consumption of land for development is unprecedented. Given the speed of Greater Vancouver's growth and its limited surrounding land, the region does not have the luxury to allow for poorly planned growth. If Vancouver is to preserve its precious farmland and improve transportation choices for its residents, it has to grow smart, which means concentrating population increases in existing neighbourhoods (Northwest Environmental Watch, 2002). To discern these growth patterns, and ensure that smart growth is prevailing in the Vancouver region, satellite imagery has been shown to be an efficient and cost effective method for detecting the growth of urban environments.

The successful launch of Landsat 7 in 1999 has provided the Landsat data user community with the opportunity to utilize the data from this satellite in an enhanced pansharpened form (Forsythe, 2004). Such enhancements allow for the detection of smaller scale changes (e.g. new houses and roads, widened highways, excavated land), which were once unobservable, but prove to be of great importance to urban planning and monitoring applications.

1.5 *Purpose of Research*

The purpose of this research is to utilize pansharpened Landsat 7 imagery to detect urban change in the Vancouver CMA across a three year period (1999-2002). The specific research objectives are:

(1) To detect urban change within the CMA using unsupervised classification procedures and image differencing techniques.
(2) To outline and analyze the change parameters from the quantitative and qualitative results generated (i.e. expansion and redevelopment).
(3) To assess the accuracy of the results and determine the reliability of the findings.

Chapter 2: Literature Review

The following chapter is divided into three sub-sections that cover the pertinent background information that is relevant to this research topic. Section 2.1 presents an overview of the Landsat satellite program with particular emphasis on the Landsat 7 platform. Section 2.2 provides a synopsis on image fusion/sharpening techniques with concentration focussed on the effectiveness of the PANSHARP fusion method. Finally, Section 2.3 summarizes past studies that have utilized remotely sensed imagery for detecting urban change and also reviews the success of the methods undertaken.

2.1 The Landsat Satellite Program Overview (1972-present)

The Landsat Program is the longest running enterprise for acquisition of imagery of the earth from space (USGS, 2004). The first Landsat satellite was launched in 1972; the most recent, Landsat 7, was launched in April 1999. A total of seven satellites compose the Landsat series (Table 2.1) with the major goal being to track land cover changes (Masek *et al*., 2000) or as Lauer *et al.* (1997) proclaim: "to discriminate, identify, categorize, and map the Earth's features and landscapes based on their spectral reflectances and emissions."

Table 2.1: Landsat satellite history and status

Satellite	Launch Date	Status
Landsat 1	July 1972	Decommissioned 1978
Landsat 2	January 1975	Decommissioned 1982
Landsat 3	March 1978	Decommissioned 1983
Landsat 4	July 1982	Data transmission problems (Standby mode)
Landsat 5	March 1984	Still collecting and transmitting data to ground stations
Landsat 6	October 1993	Failed to achieve orbit
Landsat 7	April 1999	Still collecting and transmitting data to ground stations, but since May 2003, Scan Line Corrector (SLC) problems have adversely affected imagery

Source: After Lauer *et al.*, 1997

Throughout the course of the Landsat program, the devices used to capture data have varied. Landsats 1-3 contained a Return Beam Vidicon (RBV) "camera" as well as a Multispectral Scanner (MSS) instrument. The MSS was onboard Landsats 1-5. With the launch of Landsat 4, a new device, the Thematic Mapper (TM) was introduced. The launch of Landsat 7 saw the introduction of the Enhanced Thematic Mapper (ETM+) (Lauer *et al.*, 1997; Forsythe, 2002). Table 2.2 outlines the various satellites and their sensor characteristics.

Table 2.2: Landsat satellites and sensor characteristics

Satellite	Sensor	Bandwidths (µm)	Resolution (m)	Satellite	Sensor	Bandwidths (µm)	Resolution (m)
Landsats 1&2	RBV	(1) 0.48-0.57	80	**Landsats 4&5**	MSS	(4) 0.5-0.6	82
		(2) 0.58-0.68	80			(5) 0.6-0.7	82
		(3) 0.70-0.83	80			(6) 0.7-0.8	82
	MSS	(4) 0.5-0.6	79			(7) 0.8-1.1	
		(5) 0.6-0.7	79		TM	(1) 0.45-0.52	30
		(6) 0.7-0.8	79			(2) 0.52-0.60	30
		(7) 0.8-1.1	79			(3) 0.63-0.69	30
Landsat 3	RBV	(1) 0.505-0.75	40			(4) 0.76-0.90	30
	MSS	(4) 0.5-0.6	79			(5)1.55-1.75	30
		(5) 0.6-0.7	79			(6)10.4-12.5	120
		(6) 0.7-0.8	79			(7)2.08-2.35	30
		(7) 0.8-0.11	79	**Landsat 7**	ETM	(1) 0.45-0.52	30
		(8) 10.4-12.6	240			(2) 0.52-0.60	30
						(3) 0.63-0.69	30
						(4) 0.76-0.90	30
						(5)1.55-1.75	30
						(6)10.4-12.5	150
						(7)2.08-2.35	30
						PAN 0.50-0.90	15

Source: modified after Geoimage, 2004.

Of particular interest to the context of this paper are the characteristics and properties of the Landsat 7 ETM+ satellite (Figure 2.1). The design of the ETM+ stresses the provision of data continuity with Landsat 4 and 5. Similar orbits and repeat patterns are used, as is the 185km swath width for imaging.

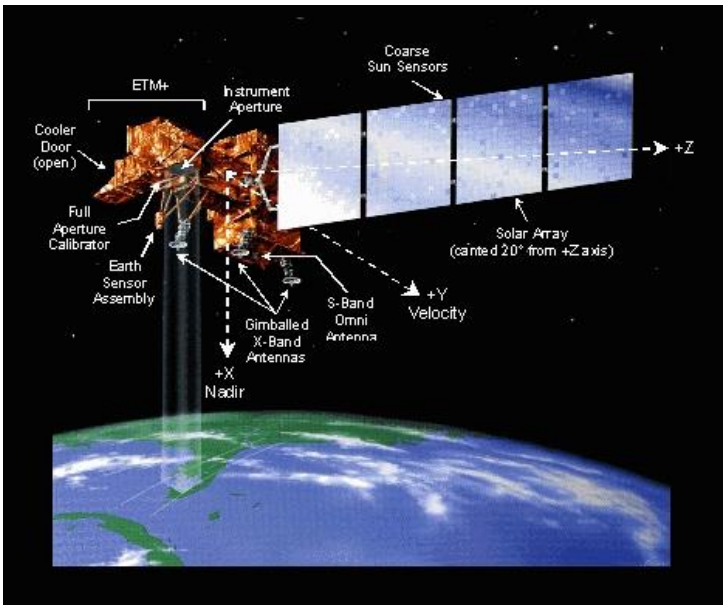

Figure 2.1: Diagram of the Landsat 7 satellite
Source: Geoscience Australia, 2004.

As with the ETM originally planned for Landsat 6, the system is designed to collect 15m resolution panchromatic data (which actually extend to 0.90µm in the near IR, well outside the visible spectral range normally associated with panchromatic imagery) and six bands of multispectral data at a resolution of 30m. A seventh, thermal band is incorporated with a resolution of 60m (versus 120m for Landsat Thematic Mapper data) - (Lillesand *et al.*, 2004).

While there have been previous satellites such as SPOT, where same-sensor image fusion was possible, with Landsat 7 the opportunity exists to enhance data over a much wider portion of the electromagnetic spectrum (Forsythe, 2004).

2.2 Image Fusion or Sharpening

Image fusion, also called pansharpening, is a technique used to integrate the geometric detail of a high resolution panchromatic image and the colour information of a low resolution multi-spectral (MS) image to produce a high-resolution MS image (Zhang, 2004). An effective image fusion technique can extend the application potential of such remotely sensed images, as many remote sensing applications require both high-spatial and high-spectral resolutions, especially for GIS based applications.

Beginning in the mid-1980's, image fusion received considerable attention from researchers in remote sensing and image processing, as the launch of SPOT 1 in 1986 provided high resolution (10m) Pan images and low resolution (20m) MS images (Zhang, 2004). Since that time, numerous academic papers on image fusion have been published to develop effective image fusion techniques, but the methods used have not always been successful or provided meaningful results. Pohl and Van Genderen (1998) referenced approximately 150 academic papers on image fusion in a review article on multisensor image fusion techniques. The emphasis in these publications has been on improving fusion quality and reducing colour distortion. Among the hundreds of variations of image fusion methods, the most popular and effective are Red-Green-Blue-Intensity-Hue-Saturation (RGB-IHS), Principal Component Analysis (PCA), Synthetic Variable Ratio (SVR), arithmetic combinations, and wavelet base fusion (Zhang 2004; Forsythe 2004). However, until now these methods were all limited by certain drawbacks. RGB-IHS transformation yields enhanced imagery, but the spectral characteristics of the data are destroyed (Cheng *et al.*, 2000). Other techniques such as PCA and SVR also provide enhanced data, but have problems, particularly with colour distortion (Forsythe, 2004).

Another common problem is that the fusion quality often depends upon the operator's fusion experience, and upon the data set being fused (Zhang, 2004). In addition, there is inevitably a difference in the time of acquisition between images obtained from different sensors. Zhang (2001) had a gap of over 2 years between Landsat TM and SPOT panchromatic data that were used for image fusion. Over this time period there would have been some land use change, causing problems with the accuracy of the fused results (Forsythe, 2004).

Currently no automatic solution has been achieved to consistently produce high quality fusion results for different datasets; however the new statistics- based PANSHARP module (implemented in the PCI Geomatica software) shows significant promise as an automated technique (Zhang, 2004). The PANSHARP method solves the two major problems in image fusion, colour distortion and operator (or dataset) dependency. It differs from existing fusion techniques in two ways. PANSHARP utilizes the least squares statistical techniques to find the best fit between the grey values of the image bands being fused and to adjust the contribution of individual bands to the fusion result to reduce colour distortion. Secondly, it employs a set of statistical approaches to estimate the grey value relationship between all input bands to eliminate the problem of dataset dependency (i.e. reduce the influence of dataset variation) and to automate the fusion process (Zhang, 2004). Due to the minimized colour distortions, maximized detail, and natural colour and feature integration, the PANSHARP method is ideal for detecting changes in an urban setting.

2.3 Strategies for Urban Change Detection Analysis and Remote Sensing Imagery

The basic premise in utilizing remotely sensed imagery for change detection analysis is that changes in the objects of interest will result in changes in reflectance values or local textures which are separable from changes caused by other factors such as differences in atmospheric conditions, illumination, viewing angles, and soil moisture. Regional land cover changes brought about by human activity tend to occur incrementally, and it can be difficult for communities to realize the extent of their development and therefore, the changes in their environment (Arthur *et al.*, 2000).

In the past, the majority of remote sensing applications were concerned with natural area management when looking at land use changes. Recently however, a trend has emerged toward the analysis of urban environments as platforms such as Landsat 7 can provide the detail required (i.e. building characteristics) which were unobservable using 80m Multi-spectral Scanner (MS) and 30m Thematic Mapper (TM) data (Forsythe, 2004).

A variety of landcover change detection techniques exist for satellite imagery, but varying levels of success have been achieved. The accuracy of change detection results depend on many factors, which include:

(1) precise geometric registration between multi-temporal images,
(2) calibration or normalization between multi-temporal images,
(3) availability of quality ground truth data,
(4) the complexity of landscape and environment of the study area,
(5) change detection methods or algorithms used,
(6) classification and change detection schemes,
(7) analyst's skills and experience,
(8) knowledge and familiarity of the study area, and
(9) time and cost restrictions (Lu *et al*., 2003).

Because of the impacts of complex factors, different authors often arrive at different and sometimes controversial conclusions about which change detection techniques are most effective. When study areas and image data are selected for research, identifying a suitable change detection technique becomes of great significance in producing good quality change detection results (Lu *et al*., 2003).

Generally speaking, these techniques can be separated into two classes: (1) detection of changes in independently-produced classifications and (2) determining change directly from radiometry (Malila, 1980; Lambin and Strahler, 1994). Despite the success of some authors using independently produced classifications (Royer and Charbonneau, 1988), most researchers (Ridd and Liu, 1998; Masek *et al.*, 2000; Forsythe, 2004) suggest image radiometry is the best method for improved urban growth estimates. With most image analysis applications, the goal is to produce classified end products through either supervised or unsupervised methods. The problem with using either of the methods over multi-temporal periods of imagery is that the classification errors will propagate over the length of the analysis period (Masek *et al.*, 2000; Yang and Lo, 2002). It is therefore more efficient to directly use radiometry, which should be relatively constant, if the image acquisition dates are consistent (e.g. year to year) and the data are from the same satellite platform (Forsythe, 2004). Specific approaches of radiometric analysis include: band-by-band image differencing, image ratioing, change vector analysis (CVA), and vegetation index differencing. These methods have a common characteristic in that they each select thresholds to determine the changed areas over several temporal periods. It is, however, critical that suitable image bands or vegetation indices are selected and suitable threshold values are determined to ensure accurate

change detection results (Lu *et al.*, 2003). Jensen and Toll (1982) were able to detect, with reasonable accuracy, urban growth in Denver, Colorado utilizing Landsat MSS (Band 5) data. Ridd and Liu (1998) compared image differencing, regression methods, Kauth-Thomas transformation, and Chi-square transformation for urban land use change detection in the Salt Lake Valley area using Landsat TM data. They concluded TM Band 2 differencing and its regression were the best methods for producing an accurate account of urban land cover change. Stow *et al.* (1990) found that ratioing multi-sensor, multi-temporal satellite image data produced higher urban land-use change accuracy than did principal component analysis (PCA). Masek *et al.* (2000) and Johnston and Watters (1996) used MSS and TM data in a Normalized Difference Vegetation Index (NDVI) subtraction approach for successful urban change detection in Washington, D.C. and achieved accuracy figures of approximately 85%. Lyon *et al.* (1998) compared seven vegetation indices from three different dates of MSS data for land cover change detection and concluded that the NDVI technique demonstrated the best vegetation change detection.

In algebra-based change detection methods, image differencing is the most often used method (Lu *et al.*, 2001). However, different authors (Stow *et al.*, 1990; Johnston and Watters, 1996; Lyon *et al.*, 1998; Ridd and Liu, 1998; Masek *et al.*, 2000) have arrived at different conclusions with regards to which method provides the best results among the image differencing, image ratioing, vegetation index differencing, and CVA approaches, since results vary depending on the study areas and image data used as stated previously.

Chapter 3: Methodology

The proceeding five sections outline the data and methodology used in this study. Specifically, Section 3.1 describes the properties of the Landsat 7 imagery and the geographical scale employed for the analysis as well as the methodological approach followed in this study. Section 3.2 outlines the various classification inputs used for the analysis, while Section's 3.3 and 3.4 describe how the unsupervised classification and radiometric band differencing techniques were carried out. Finally, Section 3.5 outlines the processing carried out via GIS to arrive at the final change detection map.

3.1 Data

For this study, two Landsat 7 Enhanced Thematic Mapper (ETM+) images were acquired for the Vancouver CMA study area. Both images were acquired on Path 47 Row 26. The dates of image acquisition were: July 28, 1999 (Figure 3.1a) and September 22, 2002 (Figure 3.1b). Census Consolidated Subdivisions (CCS) were employed as the geographical unit of scale for the analysis. The concept of a CCS is a grouping of small census subdivisions within a containing census subdivision (CSD), created for the convenience and ease of geographic referencing (Statistics Canada, 2002). The CCS scale was deemed suitable for the scope of this study as nine CCS compose the Vancouver CMA allowing for ideal analytical discussion and visualization.

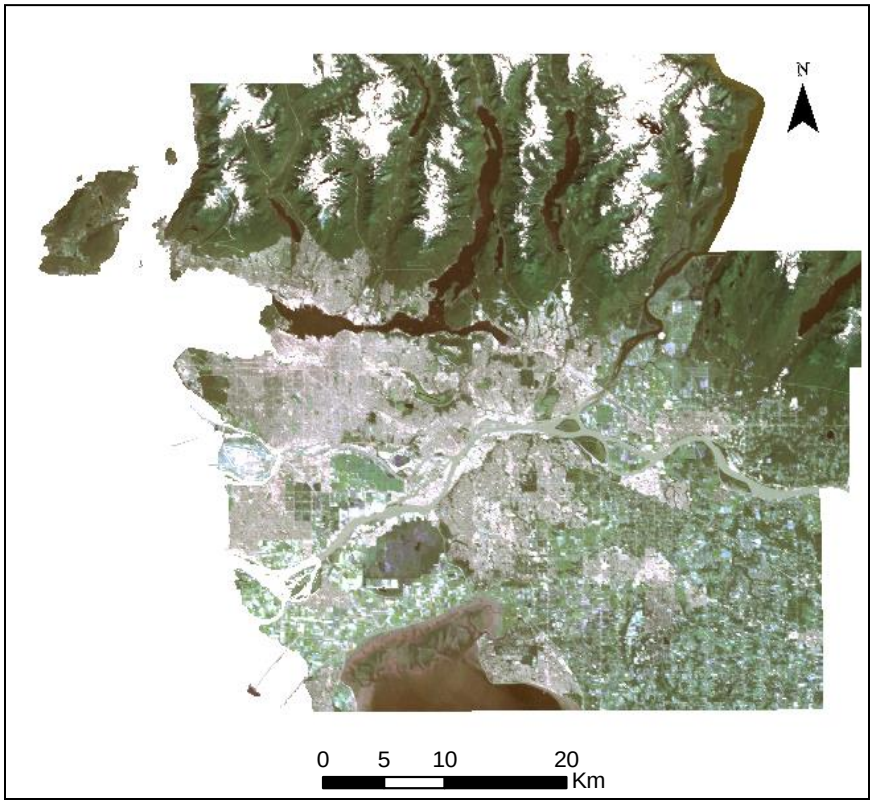

Figure 3.1a: July 28, 1999 Landsat 7 image of Vancouver CMA

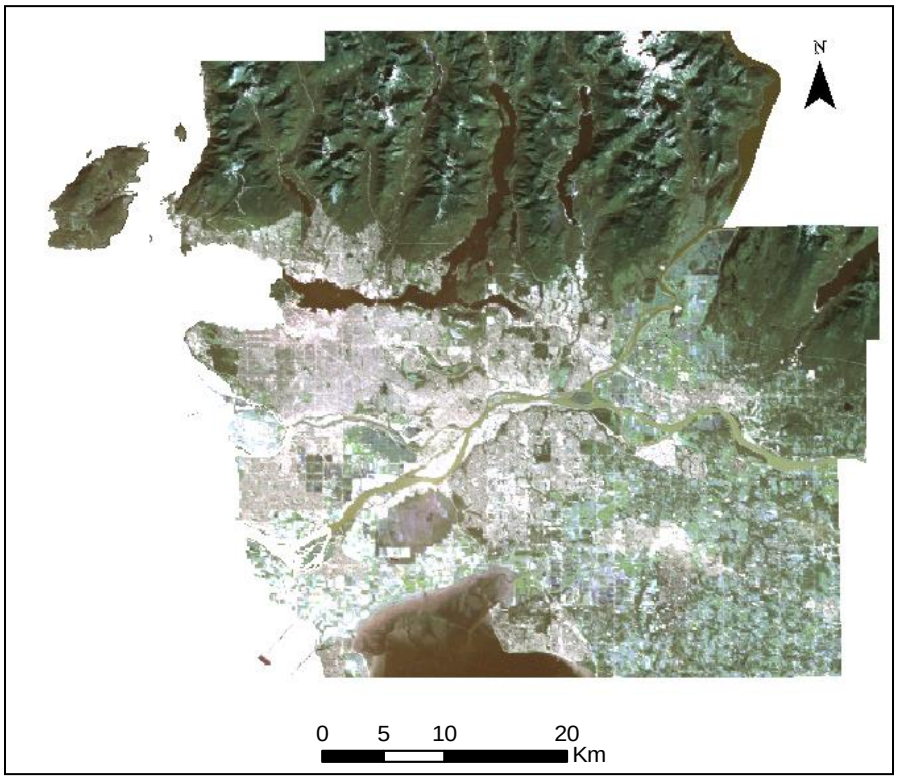

Figure 3.1b: September 22, 2002 Landsat 7 image of Vancouver CMA

Figure 3.2 conceptualizes the research approach, while the latter sections elaborate on the various methods undertaken.

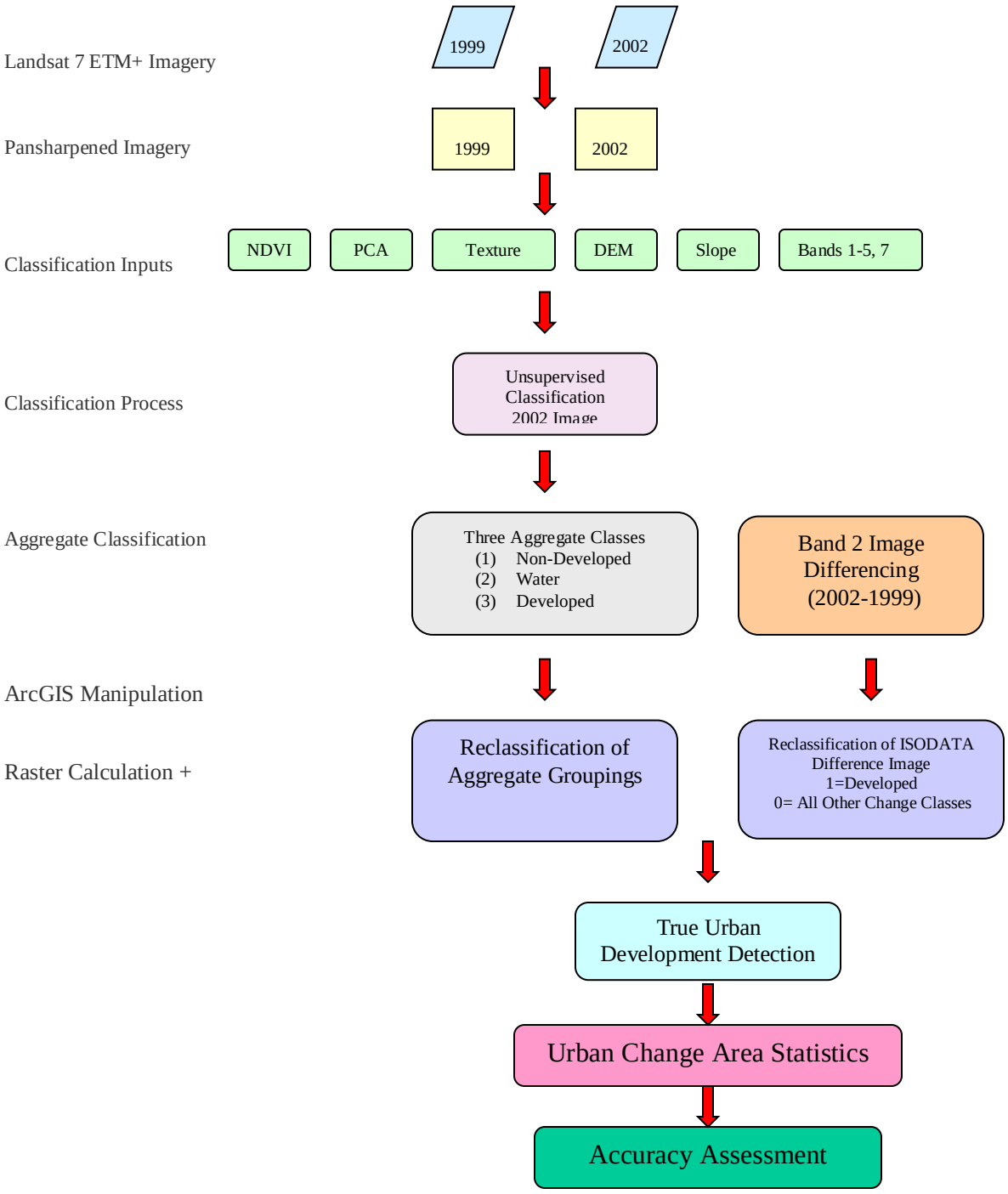

Figure 3.2: Conceptual Diagram of Research Approach

3.1.1 Pansharpened Imagery

The data fusion process was carried out using the PCI Geomatica pansharpening (PANSHARP) algorithm for the two Landsat scenes. Both images were fused (using PANSHARP) to a 15m resolution. The images were previously orthorectified to the NAD83 (GRS1980) UTM Zone 10 projection.

3.2 Classification Inputs

A combined unsupervised classification and radiometric band differencing approach was used to differentiate between true urban development and changes that occur as a result of other processes (e.g. agricultural crop rotation, crop harvesting).

3.2.1 Normalized Difference Vegetation Index (NDVI)

Spectral radiance values captured by Landsat 7's ETM+ can be analyzed independently on a band by band basis or in combinations of two or more bands. One of the most commonly used band combination techniques in vegetation studies is band ratioing (Curran 1981; Tucker 1979). In vegetation studies, the ratios, commonly known as vegetation indices, have been developed for the enhancement of spectral differences on the basis of strong vegetation absorbance in the red and strong reflectance in the near-infrared part of the spectrum. The Normalized Difference Vegetation Index (NDVI) is an index that provides a standardized method of comparing vegetation greenness between satellite images. The formula to calculate NDVI is:

$$NDVI = (\text{near IR band} - \text{red band}) / (\text{near IR band} + \text{red band})$$

Index values have been shown to range from -1.0 to 1.0, but vegetation values typically range between 0.1 and 0.7. Higher index values are associated with higher levels of healthy vegetation cover, whereas clouds and snow result in index values near zero (University of Arizona, 2002). Considering that urban expansion is often accompanied by vegetation recession, urban development information could be obtained indirectly by indexing the vegetation condition over multi-temporal periods. With respect to the Landsat ETM+, bands 3 (0.63-0.69 µm) and 4 (0.75-0.90 µm) serve as the appropriate inputs for generating the NDVI imagery for the two temporal periods. NDVI values were calculated for the two temporal periods using a NDVI algorithm developed for PCI Modeller. Figure 3.3 illustrates the NDVI results (for subsets of the images) for the two temporal periods. The subset images are intended to highlight the utility of each input for the unsupervised classification procedure. The area selected for all subset images is located in the region of Port Coquitlam, contained within the Greater Vancouver CCS. Clear differences can be depicted in this area over the three year study period which makes it an optimal location for highlighting the various layers used in the analysis.

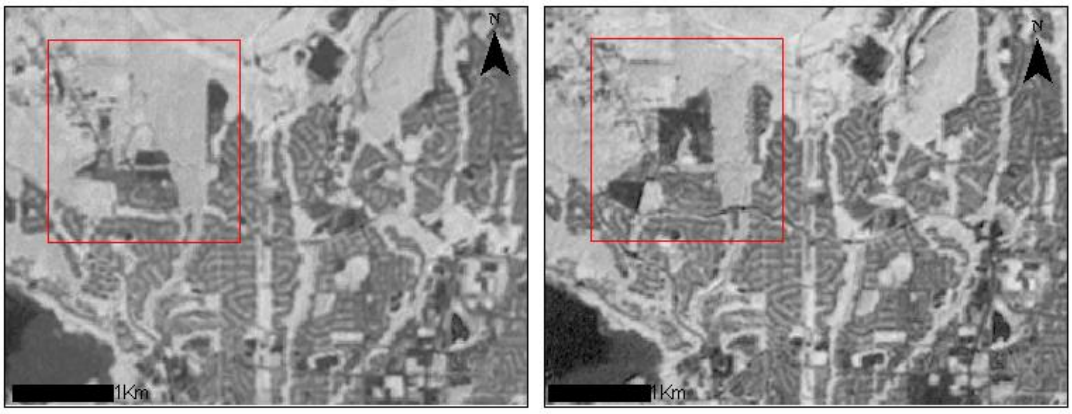

Figure 3.3: NDVI for 1999 (left) and 2002 (right)

New development is evident in the top left portion of the 2002 subset image, signified by the new dark areas representing low NDVI values. These areas are representative of new housing developments, presumably two new subdivisions located on the outskirts of Port Coquitlam. The NDVI values in the image can be directly related to the amount of photosynthetic (green) biomass within a pixel. Progressive increases from dark (black) to light (white) shades signify increasing levels of vegetation. Since urbanization in non-arid regions replaces vegetation (high NDVI) with building materials (low NDVI), sudden decreases in NDVI should indicate new urban development (Masek *et al*., 2000).

3.2.2 Principal Component Analysis (PCA)

The PCA technique is used to reduce the number of spectral components to fewer principal components which account for the most variance in multispectral images (Singh, 1989). When carried out as a pre-processing procedure prior to automated classification, PCA transformations generally increase the computational efficiency of the classification process because the PCA may result in a reduction in the dimensionality of the original dataset (Lillesand *et al.*, 2004). The first Principal Component (PC) stores the maximum contents of the variance of the original data set. The second PC describes the largest amount of the variance in the data that is not already described by the first PC, and so forth (Taylor, 1977). Although 'n' number of principal components may be acquired in the analysis, only the first few principal components account for a high proportion of the variance in the data. In some situations, almost 100 percent of the variance can be captured by these few components. Fung and LeDrew (1987) indicated that the first four components can contain more than 95 percent of the total variance and the other remaining components have little useful information for land use change.

PCA was carried out on the images using the PCA algorithm within PCI Geomatica. The first two components were utilized as they captured 99.13% of the variance within the image (Table 3.1).

Table 3.1: PCA Statistics

PC	Eigenvalue	Deviation	% Variance
1	385.2874	19.6287	96.87%
2	8.9969	2.9995	2.26%

These components serve as a valuable additional input into the classification procedure as pertinent class identification information is easily highlighted via the variance captured. Forsythe (2002) indicated that PC2 clearly illustrated newly disturbed areas for urban development in Toronto, Ontario but in this study such change was not evident. Instead, PC1 served as a better input for classification (Figure 3.4).

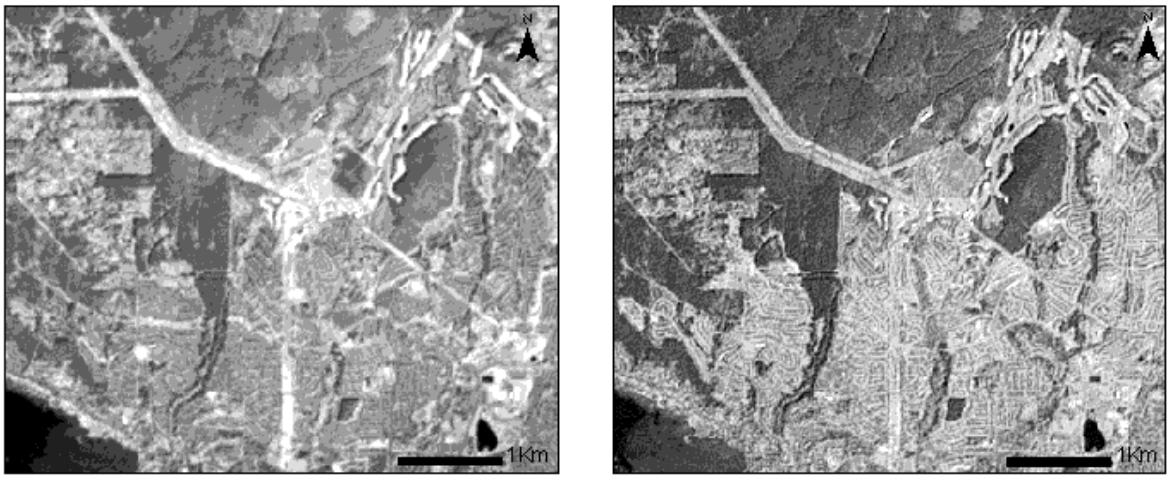

Figure 3.4: PC1 for 1999 (left) and 2002 (right)

3.2.3 Image Texture Analysis

Texture is an important characteristic used to identify objects or regions of interest in an image. Unlike spectral features, which describe the average tonal variation

in the various bands of an image, textural features contain information about the spatial distribution of tonal variations within a band (PCI, 2004). Texture is typically defined by the multidimensional variance observed in a moving window passed through an image (e.g. a 3x3 window). It is the image analyst's duty to set a variance threshold below which a window is considered "smooth" (homogeneous) and above which it is considered "rough" (heterogeneous) (Lillesand *et al*., 2004). The textural properties discerned from these windows can assist in delineating urban classes and can aid in the separation of classes where agricultural crop rotation can be mistaken for urban change (Forsythe, 2004).

Several textural trial runs were carried out utilizing various texture algorithms and window sizes (e.g. 3x3, 7x7). It was discovered that optimal results were generated via a 3x3 window (homogeneity option) performed on band 2 (Figure 3.5).

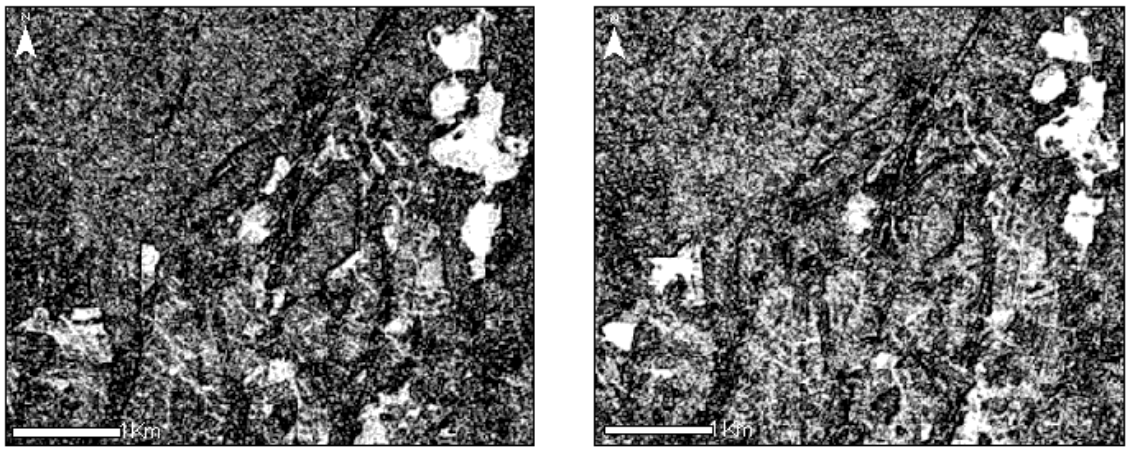

Figure 3.5: Image Texture (derived from band 2) for 1999 (left) and 2002 (right)

3.2.4 Digital Elevation Model (DEM) and Slope

DEM's and slope values are useful inputs into the classification procedure as they are able to distinguish between mountain peaks and urban areas which possess similar spectral reflectance characteristics. A 30m DEM and slope values were used as a classification input to discern these features and improve classification accuracy. The DEM was obtained through DMTI Spatial and the slope was derived using the SLOPE function in PCI Geomatica software. Figure 3.6 illustrates the extent of the DEM draped with the original 2002 pansharpened image.

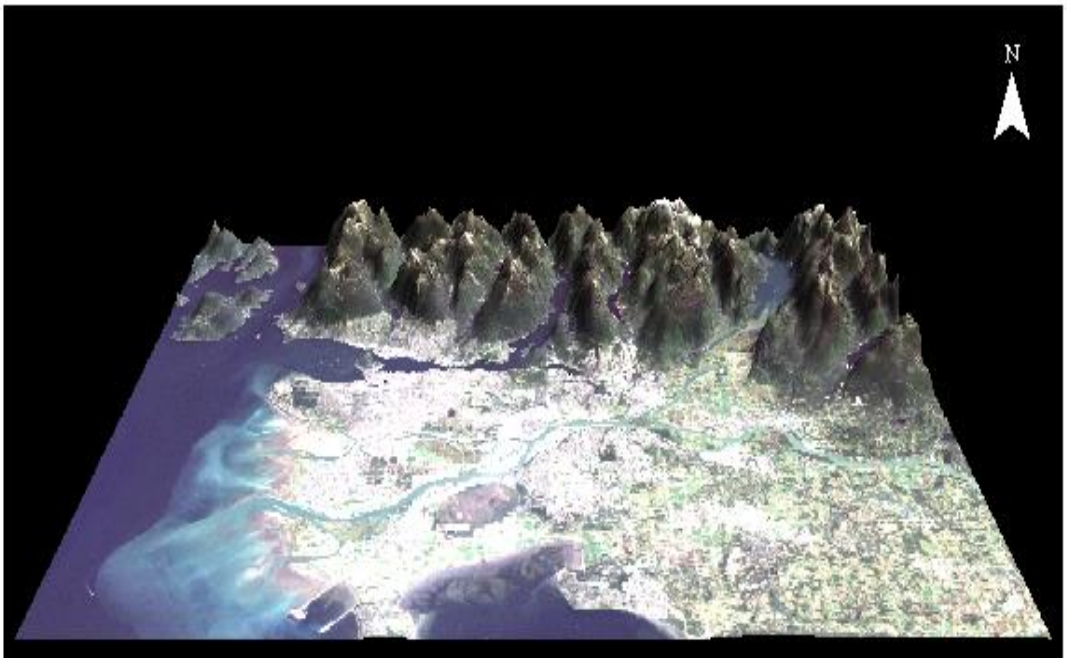

Figure 3.6: DEM draped with original 2002 pansharpened for the Vancouver CMA (Vertical Exaggeration 2.5, View Angle 45 degrees).

3.3 *Unsupervised Classification and Aggregation*

Unsupervised classification methods utilize algorithms (i.e. K-Means) that examine the unknown pixels in an image and aggregate them into a number of classes based on the natural groupings or clusters present in the image values. The basic assumption is that values within a given cover type should be close together in a multi-dimensional spectral space, whereas data in different classes should be comparatively well separated (Chen and Lee, 2001). Unlike supervised classification, the classes that result from unsupervised classification are spectral classes because they are solely based on the clusters in the image values and the identity of the spectral classes is not initially known.

An unsupervised, fuzzy k-mean classification was performed in PCI Geomatica to derive the three land cover classes. Several experimental trial procedures were carried out to determine which clustering algorithm provided the most favourable results for the images under investigation including K-means, Fuzzy K-means, and ISODATA approaches. Similar to Forsythe (2004), an unsupervised classification utilizing 255 classes proved to provide the best separation between non-developed and developed classes. Table 3.2 outlines the three classes and the layer inputs that were used for class derivation.

Table 3.2: Derived aggregate classes and layer inputs

Class	Inputs
Non-Developed	Landsat bands 5 and 7, DEM, slope, 3x3 texture, NDVI, PC1
Water	Landsat bands 1-5, and 7, DEM, slope, 3x3 texture, NDVI, PC1
Developed	Landsat bands 5 and 7, DEM, slope, 3x3 texture, NDVI, PC1

The selection of inputs for class derivation was based on the suitability of the layers to depict each land cover class. For example, Landsat bands 1-4 were not suitable for deriving the developed and non-developed classes, but proved to be very useful for generating the water class due to the inherent spectral properties. In contrast, the remaining inputs (i.e. Band 7, DEM, slope, 3x3 texture, NDVI, and PC1) provided useful information for deriving all three classes due to the geospatial and spectral information contained within each input layer.

3.4 *Radiometric Band Differencing Inputs*

One of the most widely used types of unsupervised change detection techniques is focused around the difference image. These techniques process two multi-spectral images, acquired at two different dates, in order to generate a further image. The computed difference image is one in which the values of the pixels associated with land cover changes present values significantly different from those of the pixels associated with unchanged areas (Bruzzone, 2000). Changes are then identified by analyzing (e.g. thresholding) the difference image. Two subtractive differencing operations were carried out using NDVI imagery and Band 2 data from 2002 and 1999. The resulting difference images were subjected to an ISODATA classification in which the minimum (7), maximum (10), and desired (7) change classes were selected. The resulting classified images were the optimal number of change classes determined using the ISODATA algorithm (NDVI [6], Band 2 [9]) (Figure 3.7). The classified ISODATA images were analyzed for the accuracy and consistency of detecting newly developed areas. Of note, the Band 2 difference image exhibited better results with regard to newly developed areas as more change classes were generated from the image pixels. Whereas the Band 2

difference image clearly separated developed from non-developed areas, the NDVI difference image exhibited classes containing both developed and non-developed change areas and was therefore not used in the analysis.

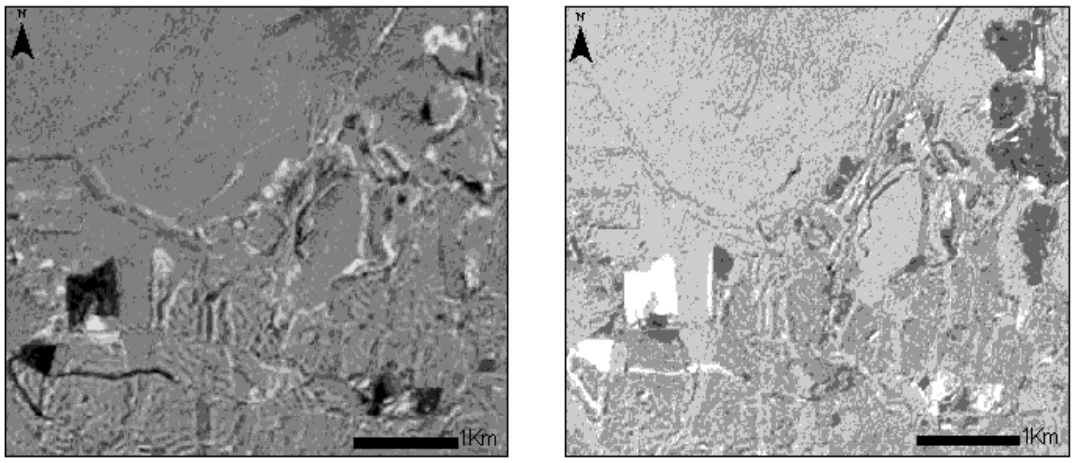

Figure 3.7 NDVI differencing for 2002 minus 1999 (left) with 6 change classes and Band 2 differencing for 2002 minus 1999 (right) with 9 change classes

The Band 2 change classes were then aggregated to isolate development from other change classes and a binary raster layer (new development =1, all other change classes = 0) was created so that overlay operations could be carried out in accordance with the aggregate 2002 image in ArcGIS.

3.5 *GIS Processing*

The classification aggregation results were exported from PCI Geomatica as Erdas Imagine (.img) files for further analysis in ArcGIS. The raster calculator was used to combine the aggregate change class results (Figure 3.7 above, Band 2) and the 2002 aggregate image (Figure 3.8). The addition of these two areas allowed for accurate urban change results. This layer was then aggregated to non-developed, water, developed, and newly developed.

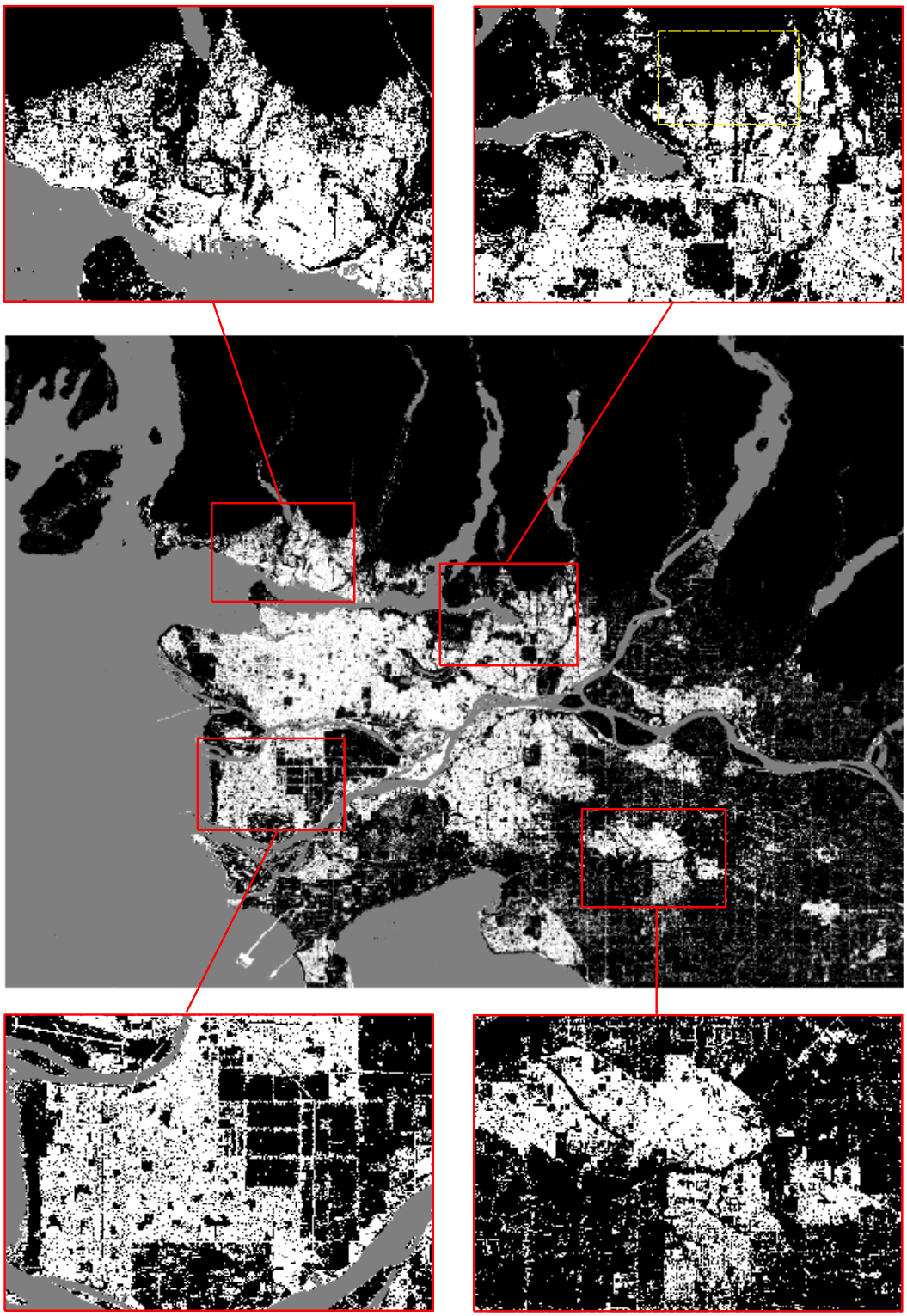

Figure 3.8: 2002 Aggregate Classification for entire analysis area (black = non-developed, grey = water, white= developed). Yellow box (Top right subset) indicates the location of the subset images from Figures 3.3, 3.4, 3.5, 3.7.

Chapter 4: Results and Discussion

The following sections discuss the results and findings of the change detection analysis. In particular, Section 4.1 highlights the area calculations for the four classes analyzed and discusses the extent of urban development in the nine CCS comprising the Vancouver CMA. Section 4.2 outlines the results of the accuracy assessments performed on the final change detection map and describes some of the discrepancies discovered in the analysis classification procedure.

4.1 Calculation of Class Areas and Development Discussion

Class Areas were determined using ArcGIS for the four land cover classes by multiplying the number of raster cells for each class by the raster resolution (15m x 15m= 225m^2) and dividing by 1000000 (1000m^2 = 1km^2). The resulting areas values for newly developed and redeveloped land are presented in Table 4.1.

Table 4.1: Class Areas: 2002-1999 (clipped to CMA boundaries)

Class Name	Area (km^2)
Non-Developed	2064.07
Water	279.16
Developed	602.57
Newly Developed	17.60

Total area analyzed: 2963.40km^2

These area parameters suggest that on average the Vancouver CMA has experienced 5.87km^2 of new development per year from 1999-2002. While this figure represents the new development that has occurred throughout the entire CMA region, a more detailed analysis of the separate CCS will highlight those areas that have experienced the most

growth during this period. The following figures depict each CCS within the CMA region using the original pansharpened imagery and aerial photography to highlight the new urban development that has occurred from 1999-2002. The pie graphs illustrate the percentage of each land class with respect to the total land area in the CCS. In addition, Table 4.2 summarizes each CCS by class area statistics.

Table 4.2: Breakdown of Class Areas (km^2) by CCS

CCS	Aggregate Classes			
	Non-Developed	***Water***	***Developed***	***New Developed***
Burnaby	39.07	7.72	65.64	0.97
Delta	123.09	75.31	59.69	3.99
Greater Vancouver	1022.40	92.21	106.06	2.95
Langley	259.31	7.50	58.13	1.87
Maple Ridge	243.50	14.91	26.36	0.82
Pitt Meadows	74.91	8.04	11.84	0.90
Richmond	69.83	9.09	55.02	1.89
Surrey	198.79	54.62	123.67	3.51
Vancouver	33.18	9.76	96.17	0.70
Total	**2064.07**	**279.16**	**602.57**	**17.60**

In Delta (Figure 4.1), the $3.99km^2$ of new development has occurred predominantly in the north-east sector and the Tilbury area as highlighted in the subset images of Figure 4.2. Evidence of new development is also clear in the Ladner and Tsawwassen areas where the majority of land transformations have been from agricultural fields to new urban development. In saying this, most change is likely a result of land excavation activities where fallow fields have been converted into land awaiting new development.

Figure 4.1: Air Photo of Delta CCS
Source: Waite Air Photos Incorporated, 2004

The region of Surrey (Figure 4.3) has also experienced ample new development, accounting for 3.51km^2 over the three year period. Overall, new development is dispersed throughout the region with considerable development arising in Guildford, Port Kells, and the south sector of the CCS (Figure 4.4).

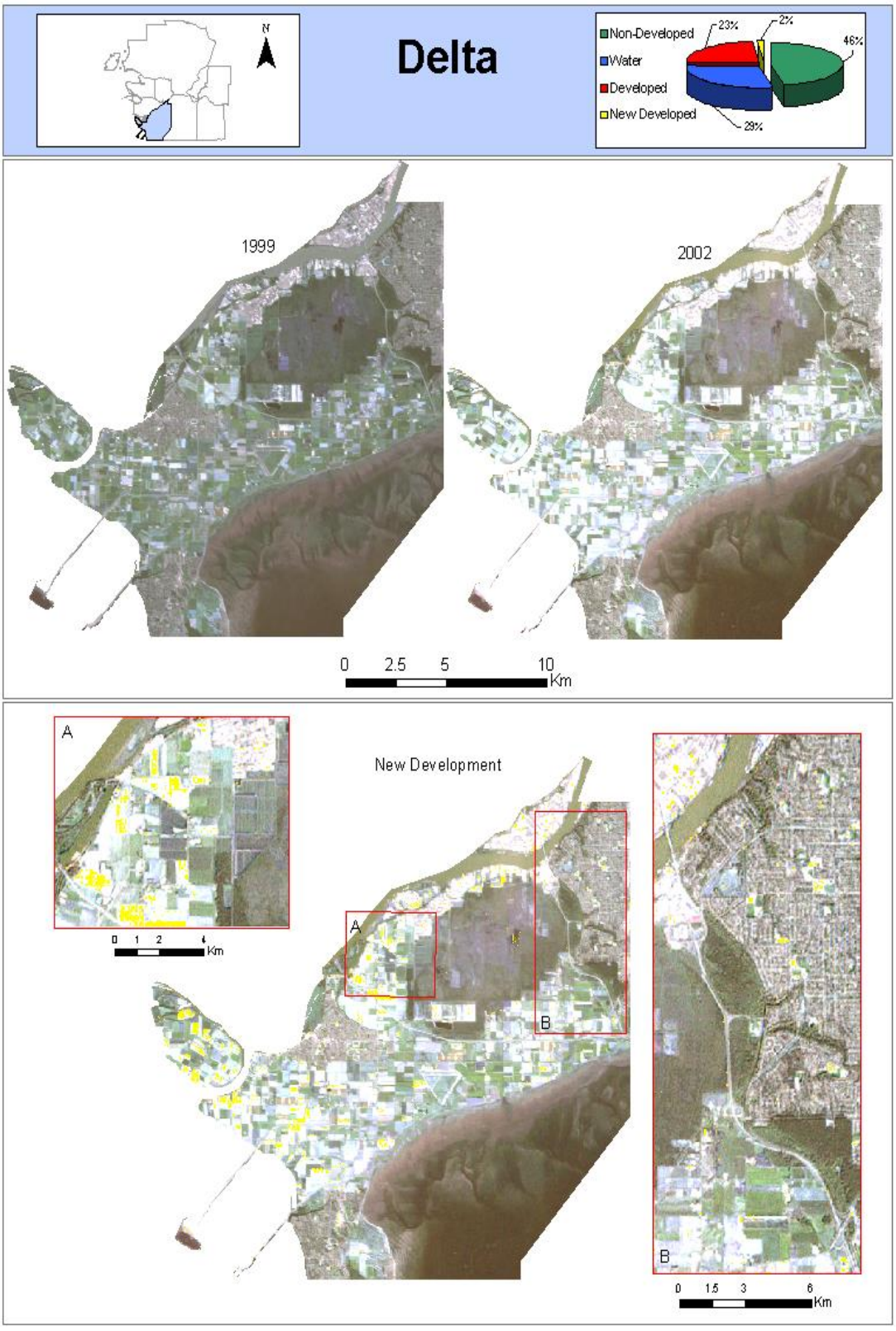

Figure 4.2: Development Results for Delta CCS

Figure 4.3: Air Photo of Surrey CCS
Source: Waite Air Photos Incorporated,

The vast region of Greater Vancouver (Figure 4.5) has experienced 2.95km^2 of new development, clearly evident in three main centres pictured in Figure 4.6. In the North Vancouver sector, newly developed areas are clearly visible in the Lonsdale and Lynn Valley areas where new areas have arisen close to the shores of the Burrard Inlet. Port Moody has been the area of choice for new development in the Greater Vancouver area with major developments occurring in the Heritage Mountain and Anmore regions.

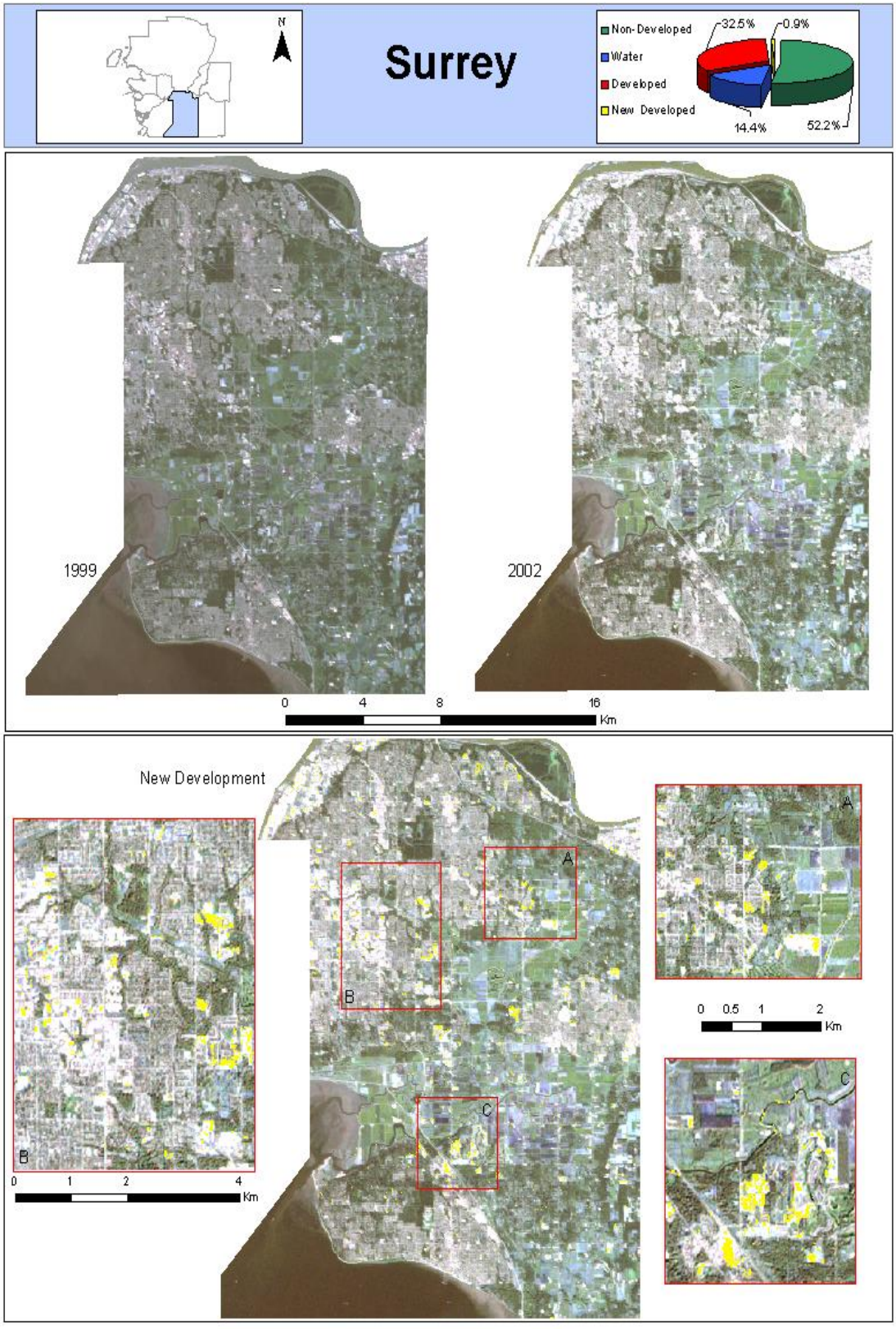

Figure 4.4: Development Results for Surrey CCS

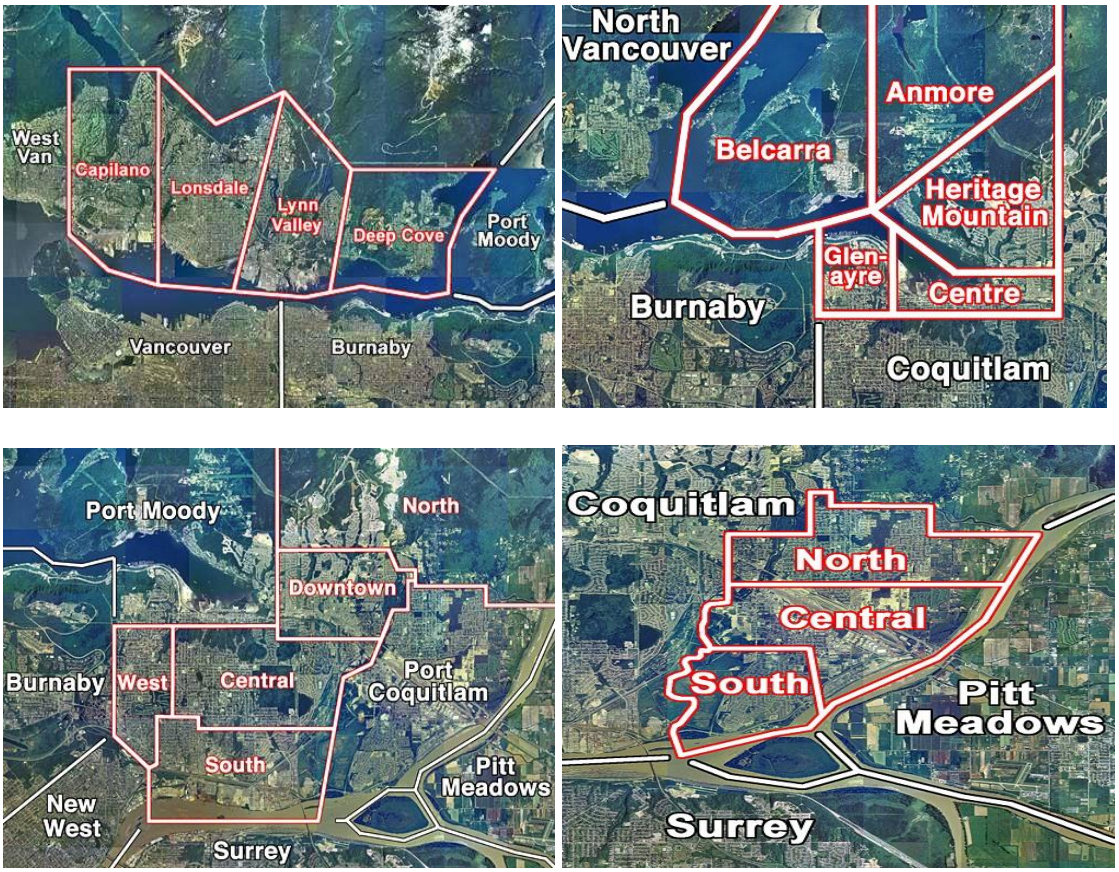

Figure 4.5: Air Photos of Greater Vancouver CCS; clockwise from top left- North Vancouver, Port Moody, Port Coquitlam, Coquitlam.
Source: Waite Air Photos Incorporated, 2004

In addition, the regions of Port Coquitlam and Coquitlam have also boasted newly developed urban areas. Most notably, the downtown area and southern portion of Coquitlam have seen development occur, as well as the central region of Port Coquitlam.

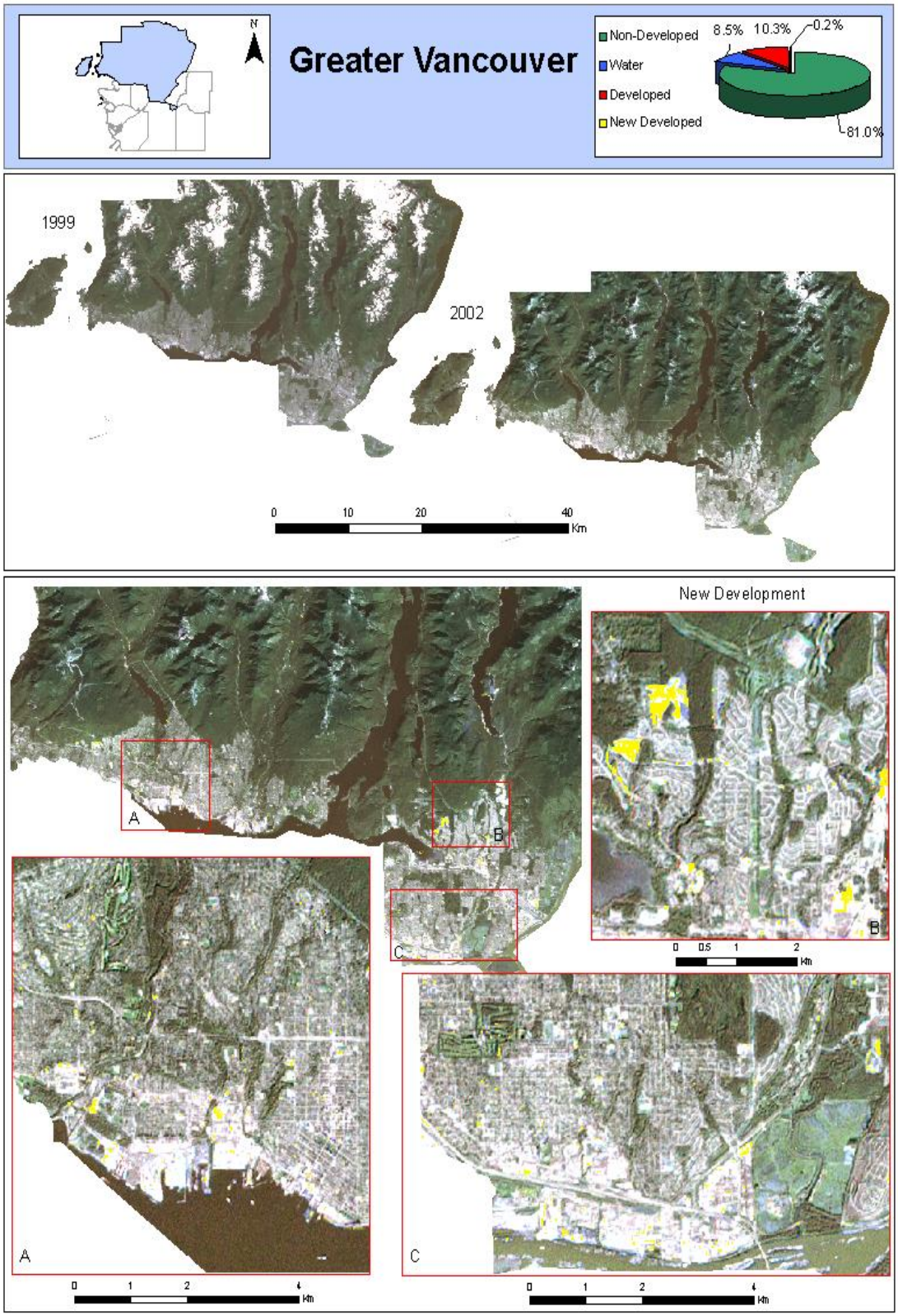

Figure 4.6: Development Results for Greater Vancouver CCS

The CCS of Richmond (Figure 4.7) has also experienced considerable development, adding approximately 1.9km^2 from 1999-2002. Generally speaking, the majority of newly developed areas have occurred in the North, East, and South sectors of the area (Figure 4.8). In contrast, the West sector and Town centre areas have experienced little development as a result of the dense urban landscape that already exists. Notably, some expansion can also be seen at Vancouver International Airport which has seen additional buildings added to the existing terminal centre.

Figure 4.7: Air Photo of Richmond CCS
Source: Waite Air Photos Incorporated, 2004

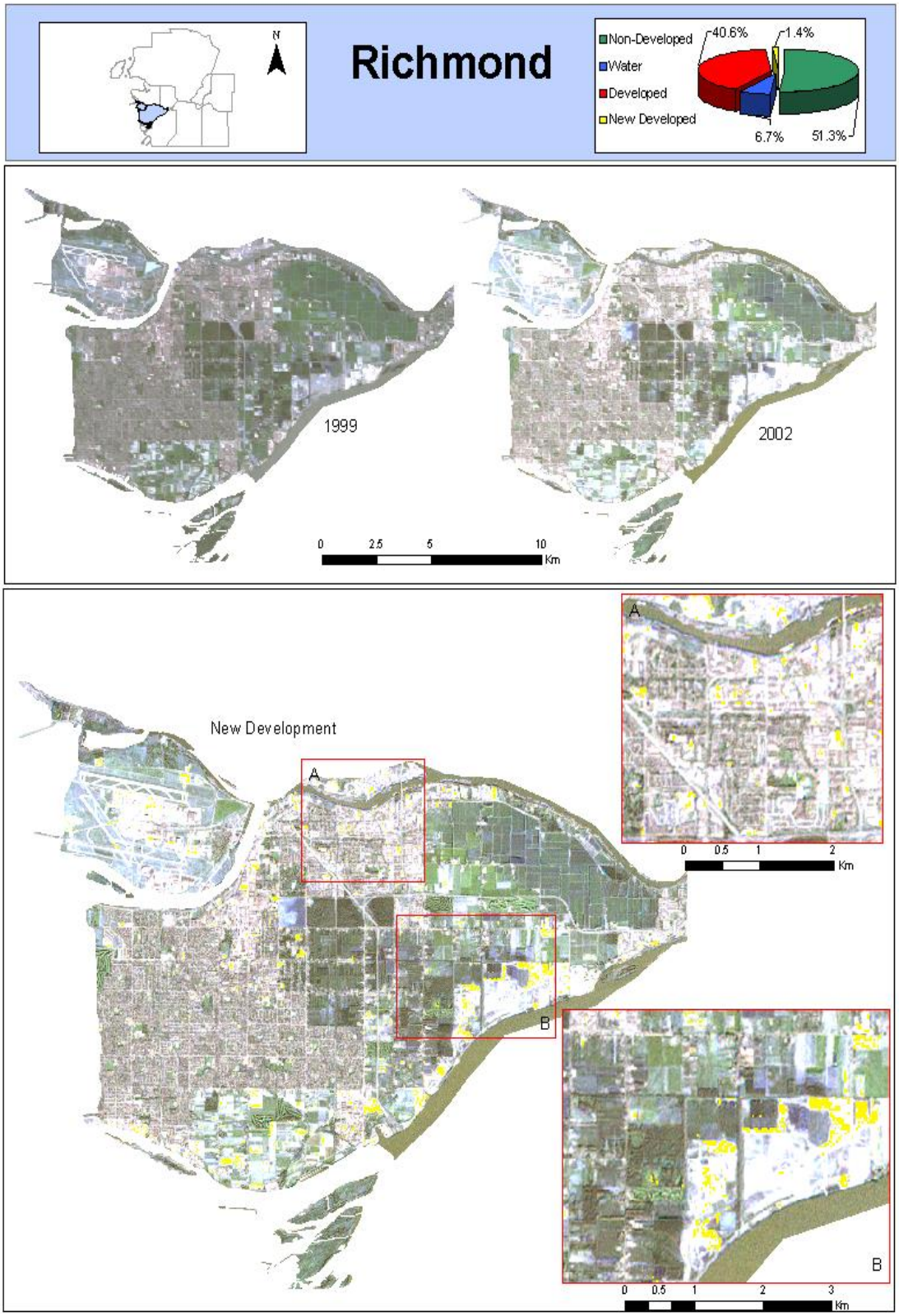

Figure 4.8: Development Results for Richmond CCS

The Langley region (Figure 4.9) has also seen development throughout the region, adding 1.87km^2 over the study period. Most notably, newly developed areas are evident in Langley City to the East and the regions of Glen Valley and Aldergrove to the west (Figure 4.10). In particular, immense development can be witnessed in the Glen Valley/ Gloucester Estate region where an apparent new subdivision has been added to the landscape in the south-eastern portion.

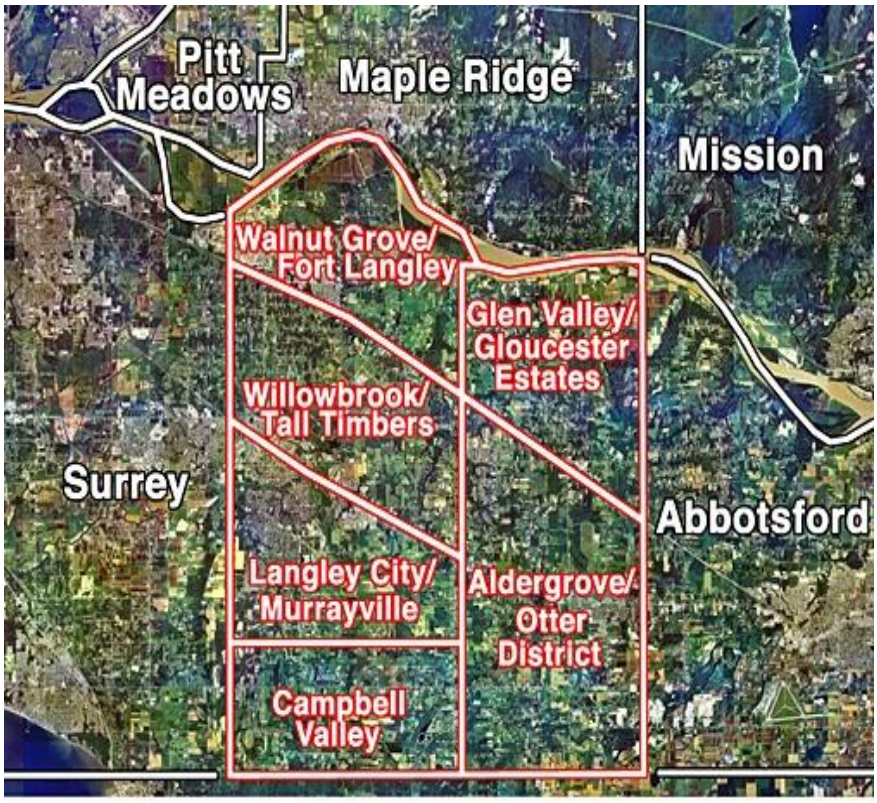

Figure 4.9: Air Photo of Langley CCS
Source: Waite Air Photos Incorporated, 2004

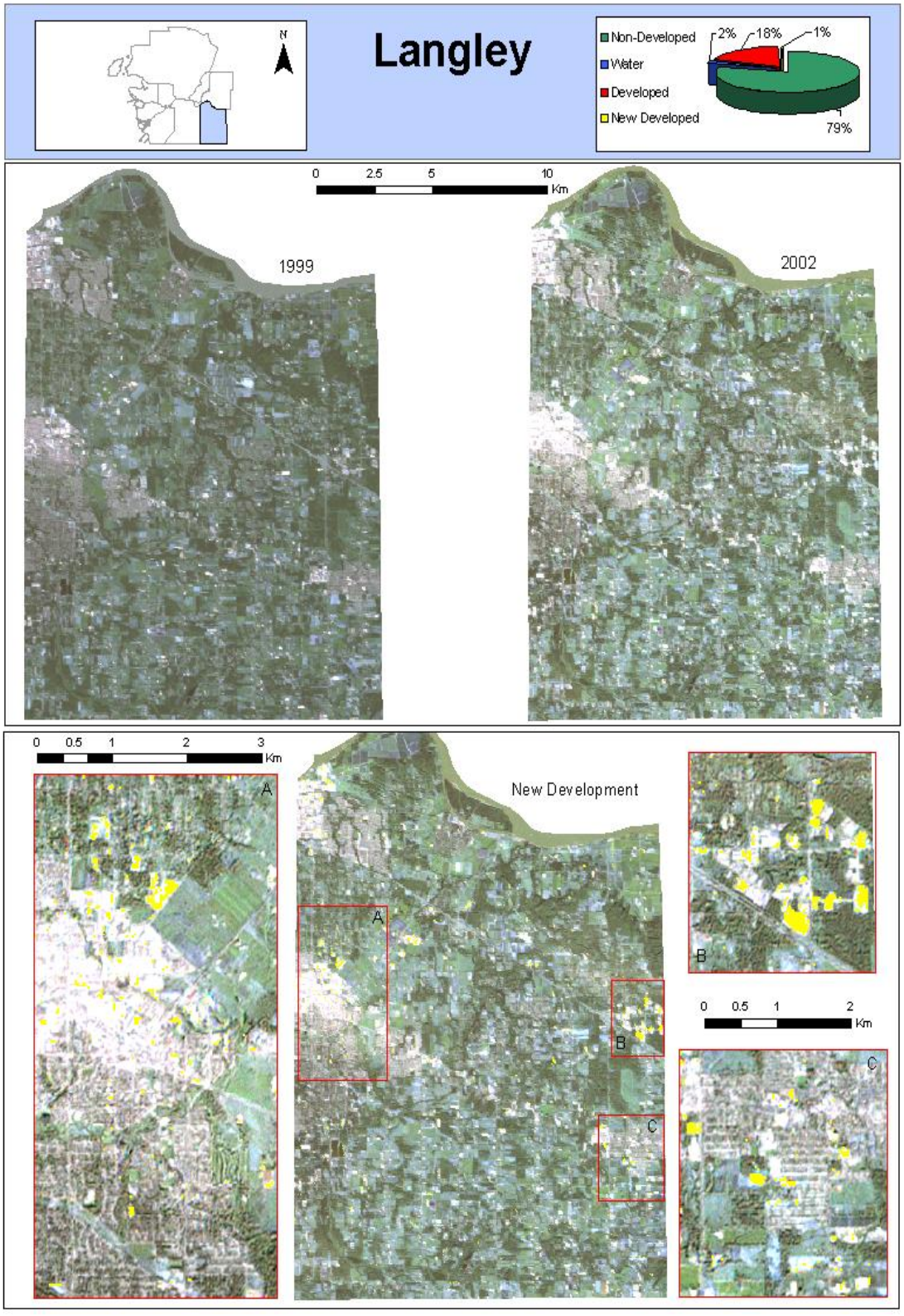

Figure 4.10: Development Results for Langley CCS

In contrast to the above mentioned CCS regions, the areas of Burnaby, Pitt Meadows, Maple Ridge, and Vancouver have experienced very little development between the subsequent years mentioned. Combined, these regions account for only 19% of the total developed area in the Vancouver CMA.

Burnaby (Figure 4.11) experienced the majority of development in the Big Bend and University & Lake City areas (Figure 4.12), resulting in 0.97km^2 of newly developed land. Similarly, the Pitt Meadows region (Figure 4.13) only experienced newly developed land in its Downtown and Western sectors (Figure 4.14), adding just 0.89km^2 over the three year period.

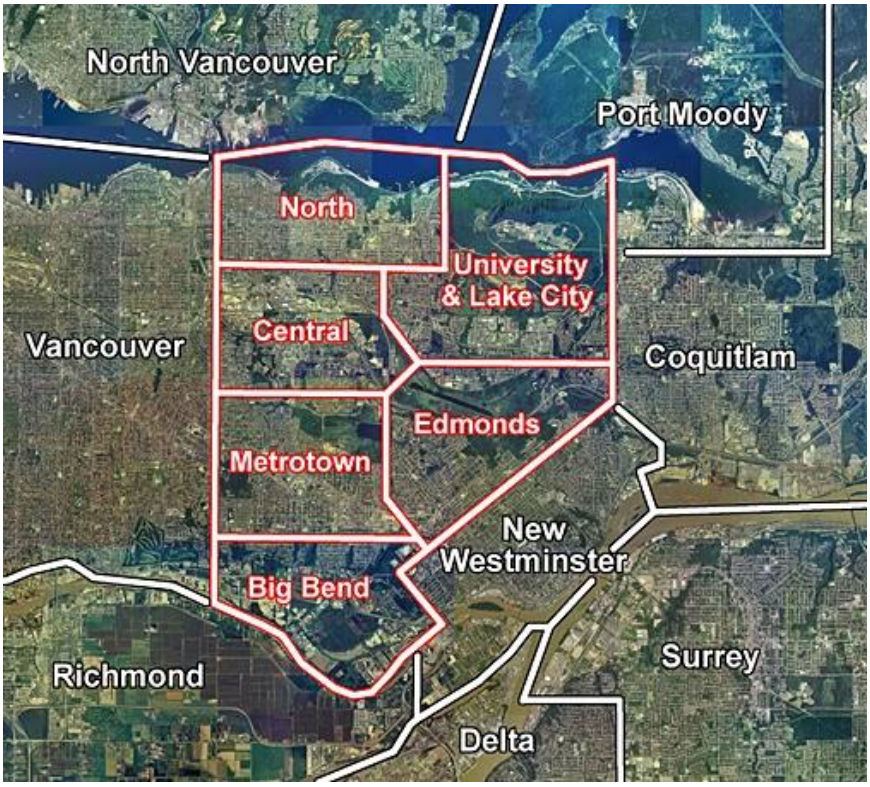

Figure 4.11: Air Photo of Burnaby CCS
Source: Waite Air Photos Incorporated, 2004

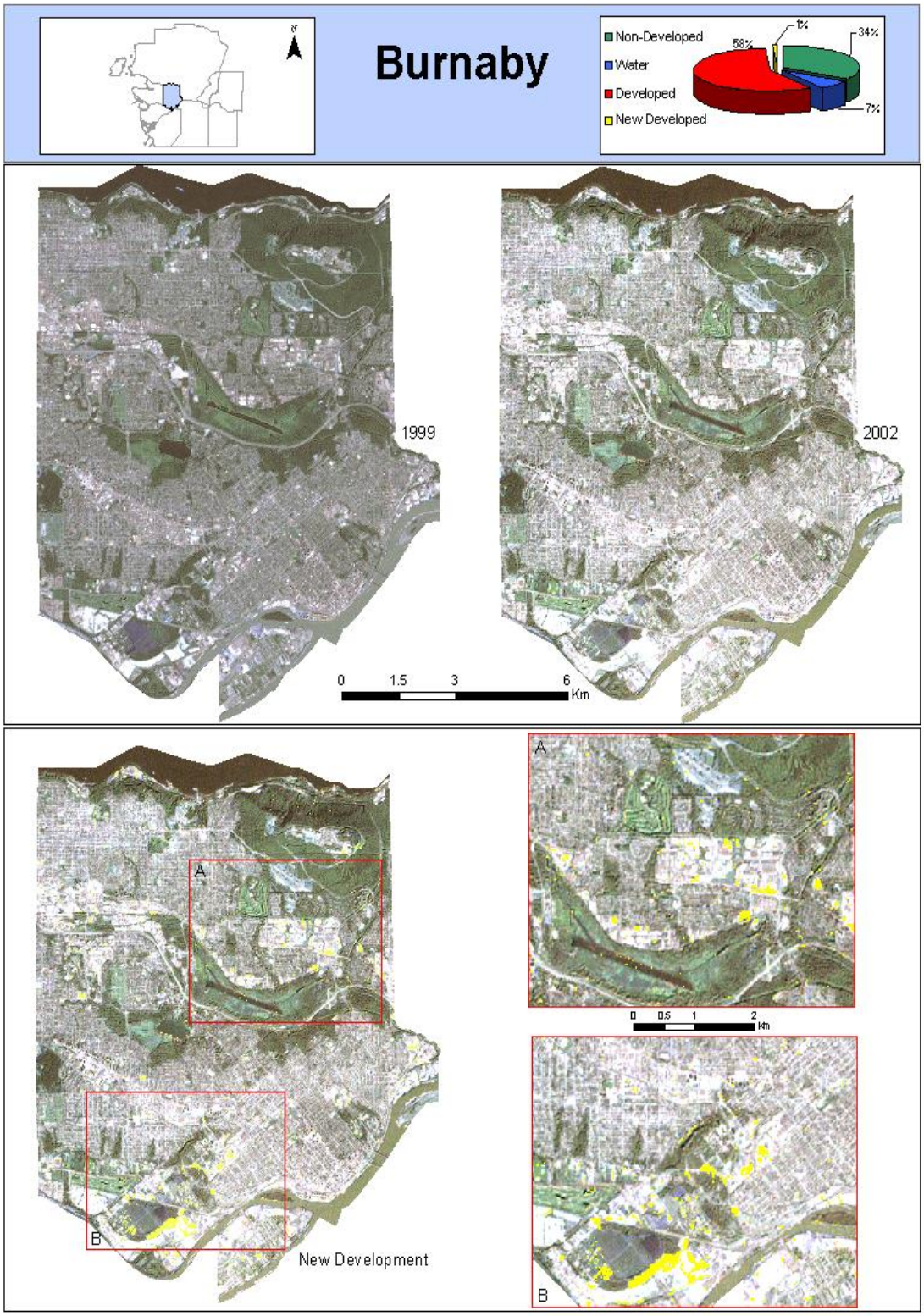

Figure 4.12: Development Results for Burnaby CCS

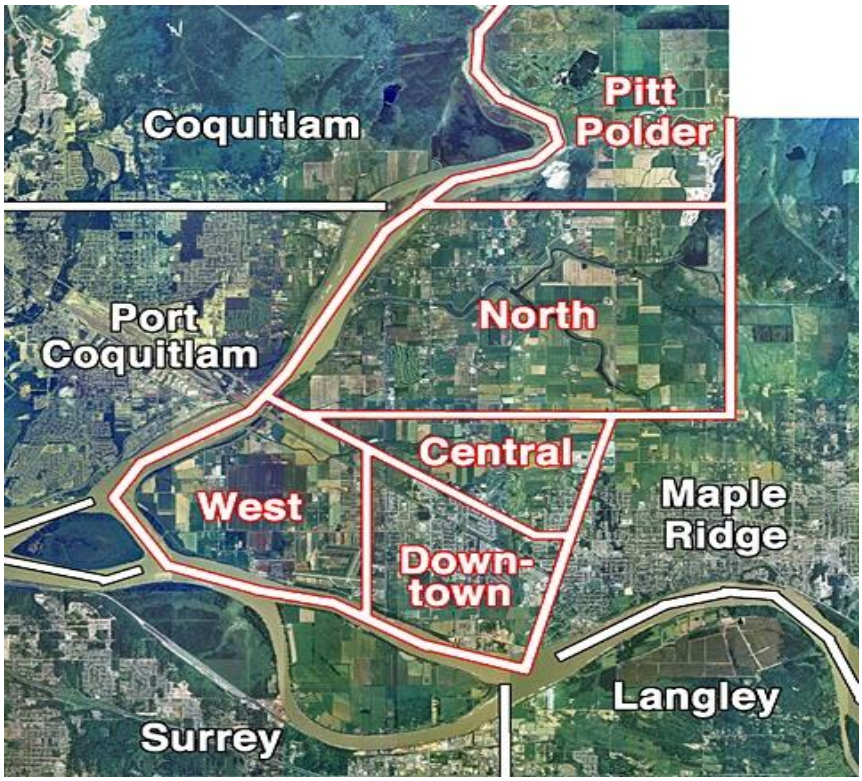

Figure 4.13: Air Photo of Pitt Meadows CCS
Source: Waite Air Photos Incorporated, 2004

Maple Ridge (Figure 4.15) experienced the second lowest amount of development (0.82km^2) over the three year period. Similar to past development patterns, newly developed areas were only evident in the West and Central sectors close to the Fraser River (Figure 4.16). Given this region is located the furthest distance from the urbanized core of Vancouver and consists of predominantly mountainous greenspace (86% of total land area), the low demand for housing does not come as a surprise as both physical and human constraints decrease development activity.

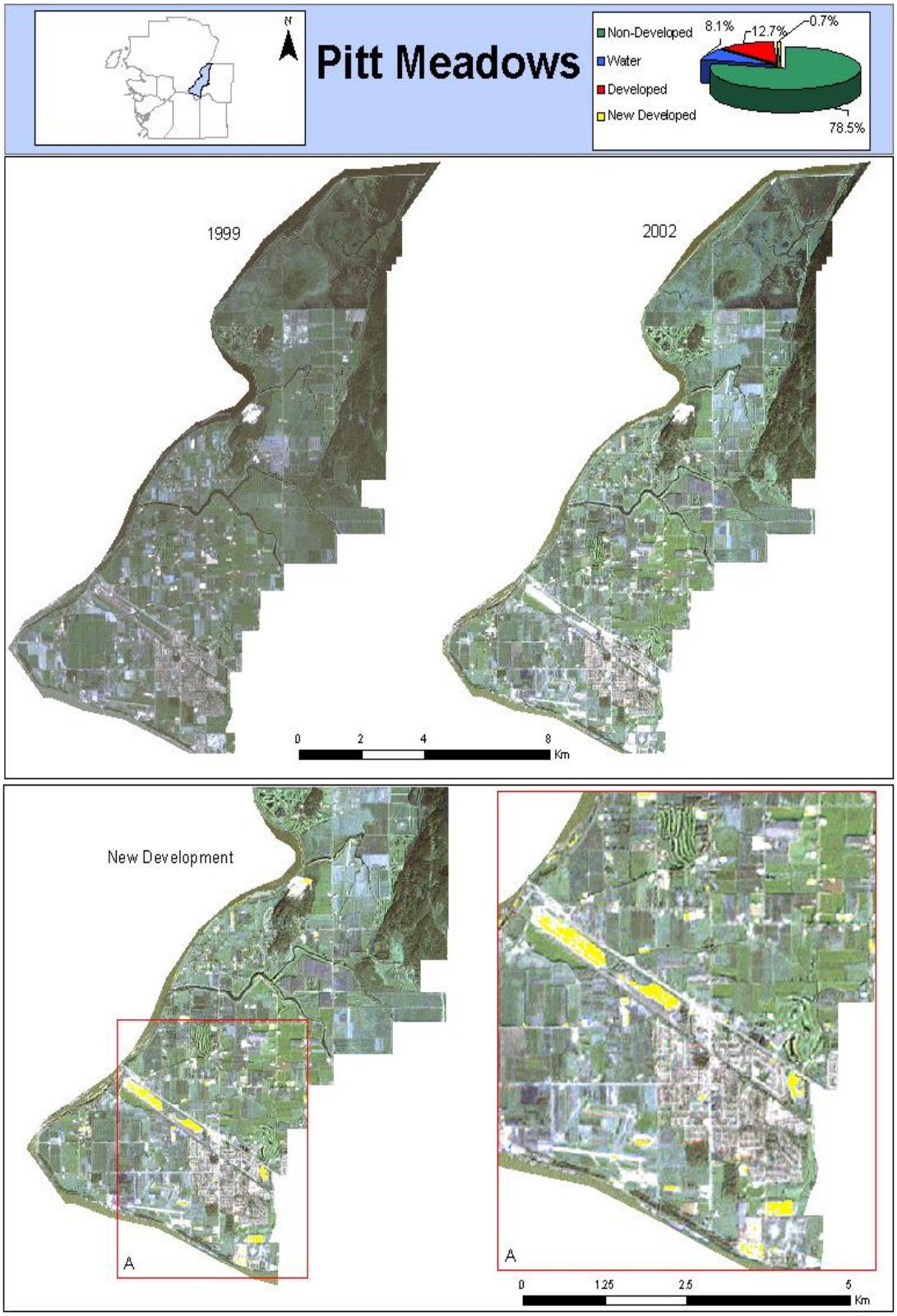

Figure 4.14: Development Results for Pitt Meadows CCS

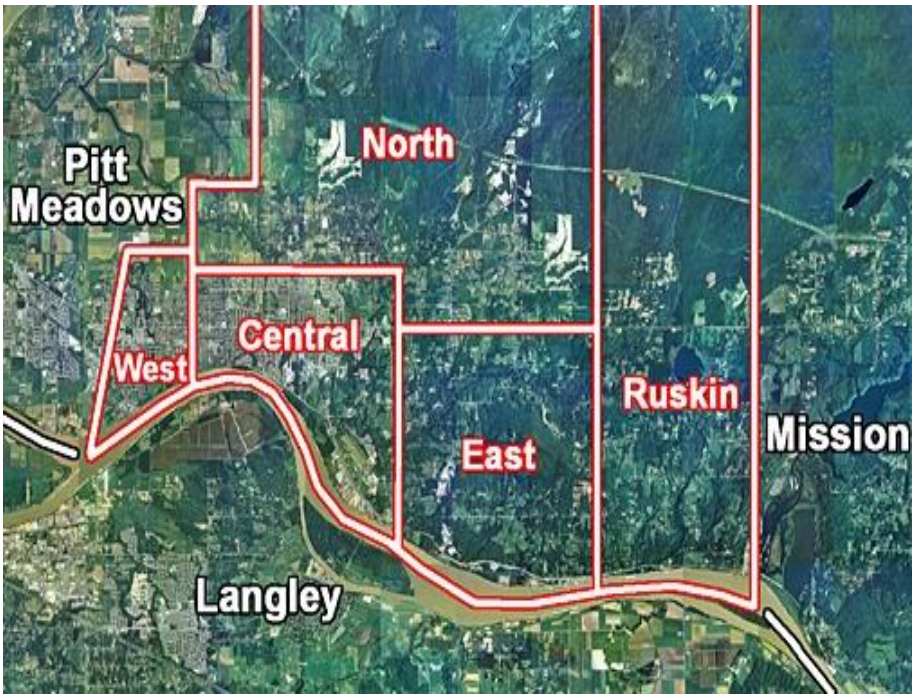

Figure 4.15: Air Photo of Maple Ridge CCS
Source: Waite Air Photos Incorporated, 2004

Finally, the heavily urbanized Vancouver region (Figure 4.17) exhibited the lowest amount of developed area in the study period, adding only 0.7km^2. Given the Vancouver region is the oldest and most urbanized area within the CMA district, such sparse development within the Central and Eastern sectors (Figure 4.18) is not surprising as little greenspace remains within the region. For this region, most development occurs in the form of redevelopment as little greenspace remains in the urbanized core of the City, with the exception of Stanley Park.

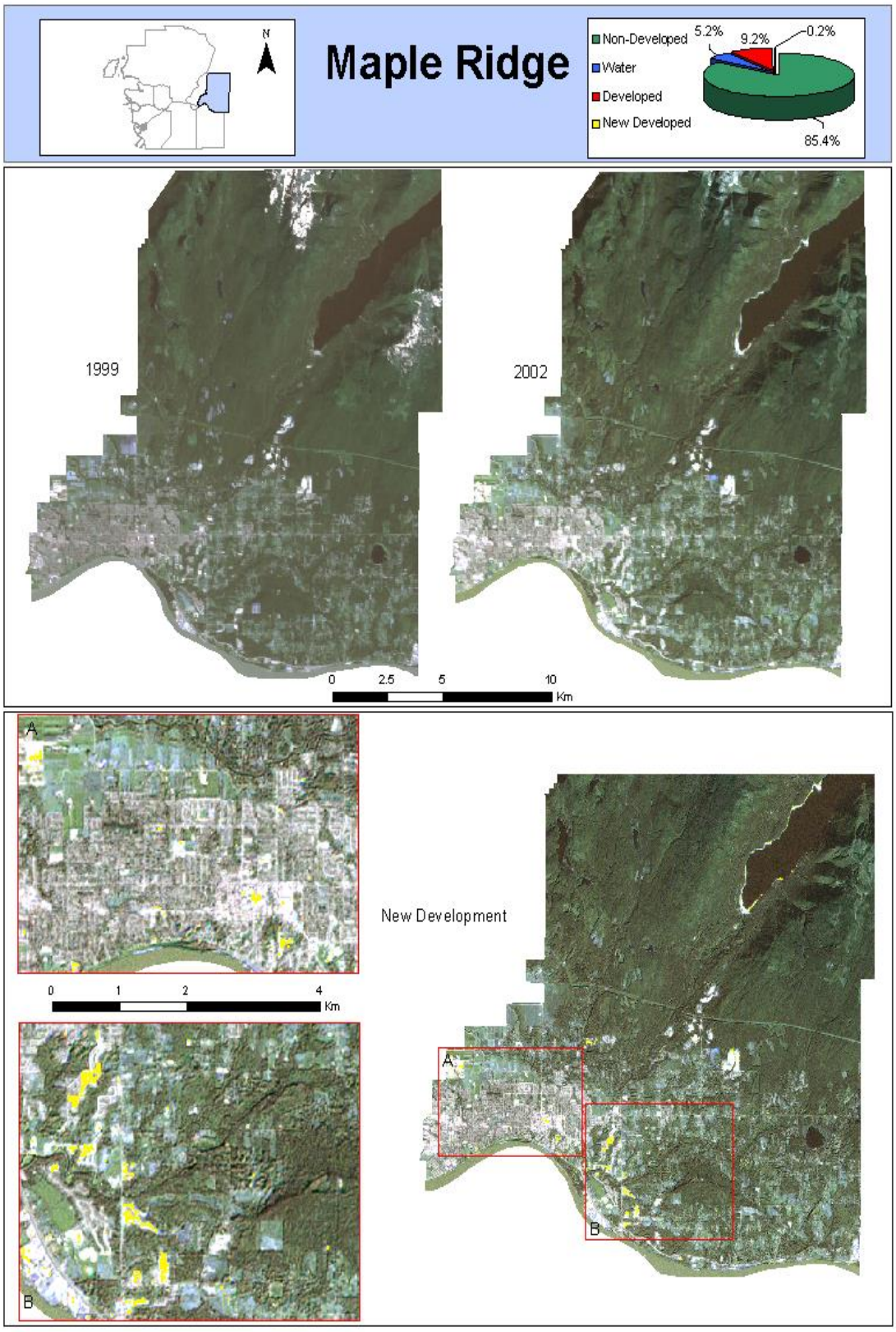

Figure 4.16: Development Results for Maple Ridge CCS

Figure 4.17: Air Photo of Vancouver CCS
Source: Waite Air Photos Incorporated, 2004

Overall, it is clear that the growth of developed areas throughout the CMA is not uniform. In fact, the majority of new growth from 1999-2002 occurred in only three of the CCS regions. While this unequal pattern may appear troublesome to some individuals, it is in direct accordance with the area's Strategic Plan for the coming years; concentrating a large share of population, and correspondingly new housing, in the Burrard Peninsula, the North East Sector, North Surrey and North Delta which is evident in the above figures. In saying this, these growth patterns not only illustrate that growth is being concentrated in a sustainable manner, but new urban development is not encroaching on the region's valuable greenspace areas.

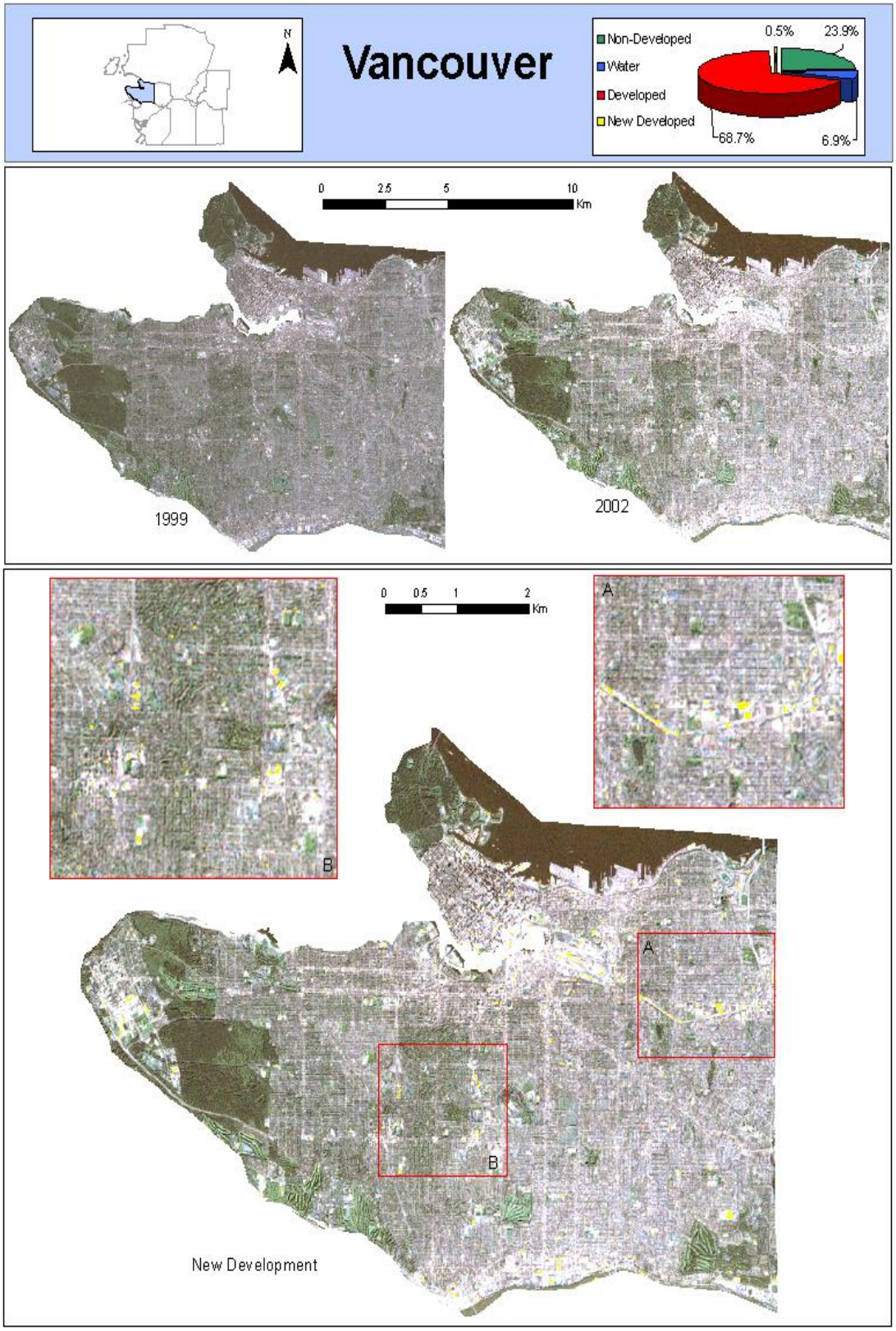

Figure 4.18: Development Results for Vancouver CCS

4.2 *Accuracy Assessment*

Classification accuracy analysis is one of the most active research fields in remote sensing. It is always claimed in the remote sensing community that a classification is not complete until its accuracy is assessed (Lillesand *et al.*, 2004). One of the most common methods of expressing classification accuracy is the preparation of a classification error matrix (or confusion table). The error matrix compares the relationship between the known reference data (based on pixel values) for each cover class and the corresponding results of the classification. Accuracy statistics are generated for each class based on the consistency of the classified image and the known pixel values for each class to be in accordance with one another.

An accuracy assessment was performed on the aggregate classification to determine the reliability of the results generated. To ensure equal distribution of sampling points within each class, 100 points were generated for the non-developed, water, and developed classes and saved as separate vector files. The resulting vector segments were then merged using the VECMERG algorithm within PCI Geomatica to arrive at the 300 point sample. Table 4.3a and b outline the accuracy statistics.

Table 4.3a: Accuracy Statistics

Overall Accuracy: 89.333%- 95% Confidence Interval (85.674% 92.993%)
Overall Kappa Statistic: 0.839% - Overall Kappa Variance: 0.001%

Class Name	Producer's Accuracy	95% Confidence Interval	User's Accuracy	95% Confidence Interval	Kappa Statistic
Non-Developed	87.96%	(81.36% 94.56%)	84.07%	(76.88%91.26%)	0.7511
Water	98.02%	(94.81%101.23%)	99.00%	(96.55%101.45%)	0.9849
Developed*	81.32%	(72.76%89.88%)	85.06%	(76.99%93.12%)	0.7855

Table 4.3b: Accuracy Statistics- Error (Confusion) Matrix

Classified Data	Reference Data			Totals
	Non-Developed	Water	Developed	
Non-Developed	95	1	17	113
Water	1	99	0	100
Developed*	12	1	74	87
Totals	108	101	91	300

*Includes developed and newly developed classes

Because the newly developed class exhibited a relatively small areal extent, with respect to the other classes, it was grouped with the existing developed class to ensure that enough random sampling points were generated for each class. Significantly, notable discrepancies were evident in the developed class where 17 of the 91 sampling points were misclassified as non-developed land. In general, these misclassifications are attributed to two main factors. Firstly, discrepancies were evident between crop rotation/harvesting practices and newly developed areas as they possessed similar spectral signatures. Most notably, the 2002 aggregate classification exhibited discrepancies in the Delta and Richmond areas where agricultural practices were in some cases mistaken for new urban development. This disparity is a clear result of the two month period separating the July and late September acquisition dates and the varying agricultural regimes that occurred between these dates. Secondly, the immense and sudden changes in topography throughout the CMA region also proved to be a problem in classification procedures. Snow laden mountain slopes exhibited very similar spectral properties as flat urban areas. Despite the use of the DEM and slope layers, misclassification was unavoidable in some instances and some areas that were obviously non-developed were grouped with the developed class. However, despite these discrepancies, the classified image represented the area quite well overall and the

accuracy figure of almost 90% illustrates the effectiveness of pansharpened imagery for land cover classification procedures. The 90% overall accuracy figure must be analyzed in relation to the individual class accuracy statistics. Most notably, the water class, with an accuracy figure of almost 100%, can be attributed to its distinct spectral values and ease of classification. The developed and non-developed classes possess accuracy values of approximately 83% and 86% respectively, and illustrate the difficulties that arise in differentiating between these two classes. While the water accuracy statistics may slightly inflate the overall accuracy figure, the accuracy of the developed and non-developed classes is still highly respectable.

Chapter 5: Conclusion

Medium and high-resolution, multi-spectral remote sensing images are an important data source for acquiring large-scale and detailed geospatial information for urban change detection studies. Landsat 7's ETM+ data, coupled with improvements to statistics-based image fusion techniques have provided the remote sensing user community with an opportunity to carry out cost effective and accurate change detection studies. Notably, pansharpened methods allow users to improve on past change detection techniques as overall classification accuracies are much higher (90-97%) than those achieved using traditional methods (75-85%). From this study, pansharpened imagery proved to be an accurate source for detecting new urban development and redevelopment in the Vancouver CMA with an overall classification accuracy of approximately 90%. In addition, the ease of implementation into a GIS for further analysis using reclassification and binary calculation procedures further signifies the utility of pansharpened imagery for change detection studies.

Overall, growth parameters and change statistics provided useful insight into the magnitude of urban change that is occurring in the Vancouver CMA area. In particular, the breakdown and discussion of each CCS comprising the CMA region was very successful in discerning new urban development and redevelopment in particular urban areas over the three year study period. The usefulness of these findings to planners and managers alike is immense. Quick and accurate growth statistics are realistic and cost-effective using pansharpened imagery and have the ability to illustrate a timeline sequence of new urban development over varying temporal periods. The ability of the pansharpened imagery to clearly depict land cover classes with tremendous spatial detail

is evident. For decision-makers, this approach can help detect where development is likely to occur based on past development patterns and current land availability. The value of this study stems from its ability to highlight the current status of urban change in the Vancouver CMA and to provide ample evidence that the region's growth strategy is being followed for the three year period under investigation.

With the current status of the Landsat 7 satellite and its SLC problems, future studies using pansharpened imagery from this platform is unlikely. However, SPOT or other satellite data and Landsat 5 TM data could possibly be used in future change detection studies as this study provides a clear and accurate framework for future replication. Such studies would not only highlight the usefulness of this application for urban change analysis, but the findings may prove to be superior to the current techniques being carried out.

For the Vancouver CMA, what the near future holds for urban development will be directly related to the immigrant population, natural growth processes, and perhaps even the upcoming Olympics. If past population patterns return to the CMA region, a sudden influx of new arrivals could generate tremendous development throughout the CMA area. However, for the period of study investigated, the Vancouver CMA demonstrated that sustainable development is a planning concept that benefits development and the environment. Currently, planners and managers should be capitalizing on the usefulness of remotely sensed pansharpened imagery so that an accurate snapshot of development patterns can be captured and new policies formulated based on accurate pansharpened results.

References

Anderson, J.R. (1977). Land use and land cover changes. A framework for monitoring. *Journal of Research by the Geological Survey*, 5; 143-153.

Arthur, S.T., T.N. Carlson, and D.A.J. Ripley. (2000). Land use dynamics of Chester County, Pennsylvania, from a satellite remote sensing perspective. *Geocarto International*, 15(1).

Atkinson, P.M. and N.J. Tate (Eds.) (2000). *Recent advances in remote sensing and GIS analysis*. John Wiley and Sons; West Sussex, England. 273 pp.

Australian Government: Geoscience Australia. (2004). *Landsat*. Available at: http://www.ga.gov.au/acres/prod_ser/landdata.htm
Last visited: September 30, 2004.

Better Environmentally Friendly Transportation. (2003*). New Urban Form: Moving for change in transportation*. Available at: http://www.best.bc.ca/_etc/pdfs/urban_fo.pdf.
Last visited: September 30, 2004.

British Columbia Statistics: Ministry of Finance and Corporate Relations. (1997). *Regional Population Trends in BC*. Available at: http://www.bcstats.gov.bc.ca/data/pop/pop/apebc97.pdf
Last visited: September 30, 2004.

Bruzzone, L. (2000). Automatic analysis of the difference image for unsupervised change detection. *IEEE Transactions on Geoscience and Remote Sensing*, 38(3); 1171-1182.

Chen, K. (2002). An approach to linking remotely sensed data and areal census data. *International Journal of Remote Sensing*, 23(1); 37-48.

Chen, Y.Q. and Y.C. Lee. (Eds.) 2001. *Geographical Data Acquisition*. New York: SpringerWien.

Chen, S., S. Zeng, and C. Xie. (2000). Remote sensing and GIS for urban growth analysis in China. *Photogrammetric Engineering and Remote Sensing*, 66(5).

Cheng, P., T. Toutin, and V. Tom. (2000). Unlocking the potential for Landsat 7 data. *Earth Observation Magazine (EOM)*. February 2000. 28-31.

City of Vancouver (2003). *Different Population Numbers*. Available at: http://www.city.vancouver.bc.ca/commsvcs/cityplans/populationhousing/populationnumbers.htm
Last visited: September 30, 2004.

City of Vancouver (2001). *2001 Census: Population Counts*. Available at: http://www.city.vancouver.bc.ca/commsvcs/housing/pdf/2001popdwellCOUNTS.PDF
Last visited: September 30, 2004.

Curran, P.J. (1981). Multispectral remote sensing for estimating biomass and productivity. *In Plants and the Day-Light Spectrum*, edited by H. Smith. New York: Academic Press. pp. 65-99.

Demographia. (2004) *Canadian City Population Counts*. Available at: http://www.demographia.com/db-cancityhist.htm
Last visited: September 30, 2004.

Discover Vancouver. (2004) *History of Vancouver BC*. Available at: http://discovervancouver.ca/history/
Last visited: September 30, 2004.

DMTI Spatial (2004). Boundary file of Vancouver CMA.

Dueker, K. and F. Horton. (1972). Urban change detection systems: Remote sensing inputs. *Photogrammetria*, 28: 89-106

Favretto, A. and C. Jurgens. (2003). Change detection techniques applied on satellite imagery in order to delineate urban sprawl evolution in Trieste Province (North East of Italy) between 1975-1999. *Proceedings of the 4th International Symposium: Remote Sensing of Urban Areas*. June 27-29, 2003. Regensburg, Germany. 56-59 (CD ROM)

Forsythe, K.W. (2004). Pansharpened Landsat 7 imagery for improved urban area classification. *Geomatica*, 58(1), 23-31.

Forsythe, K.W. (2002). Stadtentwicklung in Calgary, Toronto, und Vancouver: Interpretation mit Landsatdaten. *Proceedings of the 14th Symposium for Applied Geographic Information Processing*, July 3-5, 2002. Salzburg, Austria. 105-110.

Fung, T., and E. LeDrew. (1987). Application of principal components analysis change detection. *Photogrammetric Engineering and Remote Sensing*, 53**,** 1649-1658.

Geoimage. (2004). *Introduction to Landsat*. Available at: http://bsrsi.msu.edu/trfic/data_portal/Landsat7doc/intro_landsat.html
Last visited: September 30, 2004.

Graphic Maps (2004). *Province of British Columbia Boundary Map*. Available at: http://worldatlas.com/webimage/countrys/namerica/province/bcz.htm
Last visited: September 29, 2004.

Greater Vancouver Regional District (GVRD) (2004). *Map overview of the GVRD*. Available at: http://www.gvrd.bc.ca/growth/pdfs/GVRD2001.pdf Last visited: September 29, 2004.

GVRD Policy and Planning Department (2004). *Regional Development Indicators*. Available at: http://www.gvrd.bc.ca/publications/file.asp?ID=704. Last visited: September 30, 2004.

GVRD Policy and Planning Department (2003). *2001 Census Bulletin #6- Immigration*. Taken from 2001 Census of Canada.

GVRD Planning Department (1998). *Demographic Bulletin*. Available at: http://www.gvrd.bc.ca/publications/file.asp?ID=662 Last visited: September 30, 2004.

GVRD Livable Region Strategic Plan. (1996). *Home is Where the Housing is*. Available at: http://www.gvrd.bc.ca/publications/file.asp?ID=662) Last visited: September 30, 2004.

Hostert, P. and E. Diermayer. (2003). Employing Landsat MSS, TM, and ETM+ for mapping 3 decades of urban change in Berlin, Germany. *Proceedings of the 4th International Symposium: Remote Sensing of Urban Areas*. June 27-29, 2003. Regensburg, Germany. 225-228 (CD ROM)

Ingram, K., E. Knapp, and J.W. Robinson. (1981). Change detection technique development for improved urbanized area delineation. *Computerized Sciences Corporation*. Silver Springs Maryland, USA.

Jensen, J.R. and D.L. Toll. (1982). Detecting residential land use development at the urban fringe. *Photogrammetric Engineering and Remote Sensing*, 48; 629-643.

Johnston, A.K. and T.R. Watters. (1996). *Assessing spatial growth of the Washington Metropolitan Area using TM data*. ASPRS Conference, Baltimore, Maryland.

Kaufmann, R.K. and K.C. Seto. (2001). Change detection, accuracy, and bias in a sequential analysis of Landsat imagery in the Pearl River Delta, China: Econometric techniques. *Agriculture, Ecosystems, and Environment*, 85; 95-105.

Lambin, E.F. and A.H. Strahler. (1994). Change-vector analysis in multi-temporal space: a tool to detect and categorize land-cover change processes using high temporal-resolution satellite data. *Remote Sensing of the Environment*, 48; 231-244.

Lauer, D.T., S.A. Morain, and V.V. Salomonson. (1997). The Landsat Program: Its origins, evolution, and impacts. *Photogrammetric Engineering and Remote Sensing*, 63(7).

Lillesand, T.M., R.W. Kiefer, and J.W. Chipman. (2004). *Remote sensing and image interpretation: fifth edition*. New York: John Wiley and Sons. 763pp.

Lu, D., P. Mausel, E. Brondizio, and E. Moran. (2003) Change detection techniques. *International Journal of Remote Sensing*, 25(12); 2365–2407.

Lyon, J. G., D. Yuan, R.S. Lunetta, and C.D. Elvidge. (1998). A change detection experiment using vegetation indices. *Photogrammetric Engineering and Remote Sensing*, 64; 143–150.

Malila, W.A. (1980). Change vector analysis: an approach for detecting forest changes with Landsat. In *Proceedings of the 6th Annual Symposium on Machine Processing of Remotely Sensed Data*, Purdue University, West Lafeyette, IN. West Lafeyette, IN: Purdue University Press; 326-335.

Masek, J.G., F.E. Lindsay, and S.N. Goward. (2000). Dynamics of urban growth in Washington D.C. Metropolitan Area 1973-1996 from Landsat Observations. *International Journal of Remote Sensing*, 21(18); 3473-3486.

Northwest Environmental Watch. (2002). *Sprawl and smart growth in Greater Vancouver*. Available at:
http://www.northwestwatch.org/press/vancouver_sprawl.pdf
Last visited: September 30, 2004.

PCI Inc. (2003). *PCI Help Menu*. Richmond Hill, Ontario.

Pohl, C. and J.L. Van Genderen. (1998). Multisensor image fusion in remote sensing: Concepts, methods, and application. *International Journal of Remote Sensing*, 19(5); 823-854

Ridd, M.K. and J. Liu. (1998). A comparison of four algorithms for change detection in an urban environment. *Remote Sensing of the Environment*, 63; 95-100.

Rocky Mountain Institute (2003). *Envisioning a sustainable Vancouver*. Available at:
http://www.rmi.org/sitepages/pid1061.php
Last visited: September 30, 2004.

Royer, A. and L. Chanbonneau. (1993). Analysis of different methods for monitoring the urbanization process. *Geocarto International*, 1; 17–25.

Singh, A. (1989) Digital change detection techniques using remotely sensed data. *International Journal of Remote Sensing*, 10; 989–1003.

Statistics Canada. (2002). *Standard Geographical Classifications: Abbreviations and Hierarchical Structure*.

Statistics Canada. (1996). *1996 Census of Canada: Vancouver Population Counts*.

Stow, D. A., D. Collins, and D. McKinsey, (1990). Land use change detection based on multi-date imagery from different satellite sensor systems. *Geocarto International*, 5; 3–12.

Taylor, P. (1977). *Quantitative Methods in Geography : An Introduction to Spatial Analysis*. Boston, Massachusetts: Houghton Mifflin Company.

Tucker, C.J. (1979). Red and photographic infrared linear combinations for monitoring vegetation. *Remote Sensing of Environment*, 8: 127-150.

United States Geological Survey. (2004) *Landsat Project Website*. Available at: http://landsat7.usgs.gov/index.php
Last visited: September 30, 2004.

United States Geological Survey (1999). *Analyzing land use change in urban environments*. Available at: http://landcover.usgs.gov/urban/info/factsht.pdf
Last visited: September 30, 2004.

University of Arizona. NDVI (2002). *NDVI*. Available at: http://rangeview.arizona.edu/glossary/ndvi.html
Last visited: September 30, 2004.

Urban Futures Institute (2003). *The next century of population growth and change: A projection of Metropolitan Vancouver's Population, 1999 to 2101*. Available at: http://www.urbanfutures.com/Institute/abstracts/report44.htm
Last visited: September 30, 2004.

Waite Air Photos (2004). *Air Photos of Greater Vancouver*. Available at: http://www.globalairphotos.com
Last visited: September 30, 2004.

Yang, X. and C.P. Lo. (2002). Using a time series of satellite imagery to detect land use and land cover changes in the Atlanta, Georgia metropolitan area. *International Journal of Remote Sensing*, 23(9); 1775-1798.

Yeh, A.G., and X. Li. (2001). Measurement and monitoring of urban sprawl in rapidly growing regions using entropy. *Photogrammetric Engineering & Remote Sensing*, 67(1).

Zhang, Y. (2004). Understanding Image Fusion. *Photogrammetric Engineering and Remote Sensing*, June 2004; 657-661.

Zhang, Y. (2001). Detection of urban housing development by fusing multisensor satellite data and performing spatial feature post-classification. *International Journal of Remote Sensing*, 22(17); 3339-3355.

Zhu, C. and X.Yang. (1998). Study of remote sensing image texture analysis and classification using wavelet. *International Journal of Remote Sensing*, 19(16); 3197-3203.

.